

Affleck-Dine Baryogenesis and Dark Matter Production after High-scale Inflation

Keisuke Harigaya,¹ Ayuki Kamada,^{1,2} Masahiro Kawasaki,^{3,1}

Kyohei Mukaida,⁴ and Masaki Yamada^{1,3}

¹*Kavli IPMU (WPI), TODIAS, University of Tokyo, Kashiwa, 277-8583, Japan*

²*Department of Physics and Astronomy,*

University of California, Riverside, CA, 92507, USA

³*ICRR, University of Tokyo, Kashiwa, 277-8582, Japan*

⁴*Department of Physics, Faculty of Science,*

University of Tokyo, Bunkyo-ku, 133-0033, Japan

(Dated: October 1, 2018)

Abstract

The discovery of the primordial B-mode polarization by the BICEP2 experiment indicates inflation with a relatively high energy scale. Taking this indication into account, we propose consistent scenarios to account for the observed baryon and dark matter densities in gravity and gauge mediated supersymmetry breaking models. The baryon asymmetry is explained by the Affleck-Dine mechanism, which requires relatively low reheating temperature to avoid a sizable baryonic isocurvature perturbation. The low reheating temperature then requires non-thermal production of dark matter to account for the correct relic density of dark matter. Our scenarios can account for the observations of baryon and dark matter density in gravity and gauge mediation and predict some parameters, including the mass of dark matter.

PACS numbers: 98.80.Cq, 95.35.+d, 11.30.Fs, 12.60.Jv

I. INTRODUCTION

Inflationary cosmology is now almost confirmed by the discovery of the primordial B-mode polarization by the BICEP2 experiment [1]. Then we confront a mystery of the origins of baryon asymmetry and dark matter (DM), which are erased by exponential expansion of the Universe during inflation. For a consistency of the inflationary cosmology, we have to account for the origin of baryon asymmetry and DM after inflation,¹ taking experimental facts into account, including the result of the BICEP2.

The recent result of the BICEP2 experiment implies inflation with a relatively high energy scale:

$$H_{\text{inf}} \simeq 1.2 \times 10^{14} \text{ GeV} \left(\frac{r}{0.2} \right)^{1/2}, \quad (1)$$

$$r = 0.20_{-0.05}^{+0.07} \quad (68\% \text{CL}), \quad (2)$$

where H_{inf} is the Hubble parameter during inflation, and r is the tensor-to-scalar ratio. To explain the origins of baryon asymmetry and DM after such a high-scale inflation, we focus on models of supersymmetry (SUSY). In these models, the lightest SUSY particle (LSP) is a good candidate for DM, and the baryon asymmetry can be explained by the Affleck-Dine mechanism [4, 5], in which a baryonic scalar field with a flat potential, called the AD field, plays an important role. However, the Affleck-Dine baryogenesis after high-scale inflation results in a sizable baryonic isocurvature fluctuation [6–9],² unless the vacuum expectation value (VEV) of the AD field is very large during inflation. The Affleck-Dine baryogenesis with such a large VEV of the AD field often requires too low reheating temperature to produce DM thermally. It is necessary to investigate a scenario for non-thermal production of DM.

Moreover, the Affleck-Dine baryogenesis usually predicts formation of a localized lump composed of condensation of scalar fields carrying enormously large baryon charge [14–19]. The lump is referred to as a Q-ball [20], which is long-lived due to the conservation of baryon charge. Q-balls emit quarks from their surfaces and release their charges into standard model particles [21]. At the same time, Q-balls may decay into light SUSY particles and be another source of DM [16, 22–32].

¹ For production of baryon asymmetry and/or DM during inflation, see Refs. [2, 3].

² Axion cold DM is also restricted by the result of BICEP2 and isocurvature constraints [10–13].

In this paper, we construct consistent scenarios to account for the observed baryon and DM densities in the cases with and without Q-ball formation in models of gravity and gauge mediation. In gravity mediation, non-thermal production of DM in a low reheating temperature has been investigated in detail in Ref. [33] (see also Ref. [34]), where DM is produced mainly by two mechanisms: direct decay of inflaton into SUSY particles [34–39] and inelastic scatterings during reheating process [33, 34]. In addition, if Q-balls are formed after the Affleck-Dine baryogenesis, DM is also produced from the decay of Q-balls [16, 22–26, 32]. In this case, since the branching fractions of the Q-ball into quarks and gauginos are related with each other by a simple relation, we may overcome the baryon-DM coincidence problem [32]. In gauge mediation, the gravitino is the LSP, which is produced by scatterings between gluinos and gluons just after the end of reheating and is thus related with the reheating temperature [40]. Besides, any flat direction other than the one contains Higgs fields results in the formation of Q-balls after the Affleck-Dine baryogenesis. Then Q-balls provide another source of gravitinos [27–31]. Although gravitinos can be directly produced from the decay of Q-balls, they are mainly produced from the next-to-lightest SUSY particle (NLSP) into which Q-balls decay. We find that these scenarios in gravity and gauge mediation can be consistent with the observations of baryon and DM densities as well as the result of the BICEP2 experiment, and have predicted some parameters, including the mass of DM.

This paper is organized as follows. In the next two sections, we calculate the baryon density and baryonic isocurvature perturbation resulting from the Affleck-Dine baryogenesis, and derive an upper bound on reheating temperature by consistency with observations. Then we briefly explain the Q-ball and its properties. In Sec. V, we construct scenarios to account for the observed baryon and DM density in the context of low reheating temperature. We consider the cases with and without Q-ball formation, in gravity and gauge mediation. Section VI is devoted to the summary and conclusion.

II. AFFLECK-DINE BARYOGENESIS

Typical SUSY models, including the Minimal SUSY Standard Model (MSSM), contain many flat directions, whose F and D term potentials are absent in renormalizable levels [41]. Such flat directions are sometimes referred to as AD fields, named after Affleck and Dine.

The following combination of an up-type right-handed squark and two down-type right-handed squarks, denoted as ϕ , is an example of a flat direction, called $\bar{u}\bar{d}\bar{d}$ flat direction:

$$\tilde{u}_1^R = \frac{1}{\sqrt{3}}\phi, \quad (3)$$

$$\tilde{d}_1^G = \frac{1}{\sqrt{3}}\phi, \quad (4)$$

$$\tilde{d}_2^B = \frac{1}{\sqrt{3}}\phi, \quad (5)$$

where subscripts and superscripts represent family indices and color indices, respectively. In this paper, we do not restrict ourselves to $\bar{u}\bar{d}\bar{d}$ flat direction, but use it as an illustration in some cases.

Let us consider classical dynamics of an AD field with B (or $B - L$) charge, such as $\bar{u}\bar{d}\bar{d}$ flat direction. During inflation, we assume that the AD field obtains a large VEV. Non-renormalizable terms, which break CP and B (or $B - L$) symmetry in general, are relevant for the dynamics of the AD field due to the large VEV. After inflation ends, the AD field starts to oscillate and rotate in the complex plane around the low energy vacuum, whose dynamics is far from thermal equilibrium. In this way, Sakharov's conditions for baryogenesis [42] are satisfied and B (or $B - L$) asymmetry is generated. Since the amplitude of the oscillation decreases due to the Hubble expansion, the non-renormalizable terms becomes irrelevant and B (or $B - L$) symmetry is approximately restored. If the AD field releases its charge into the standard model particles after the sphaleron process [43] freezes out, the AD field should have B charge to account for the baryon asymmetric Universe. On the other hand, if the AD field releases its charge before the sphaleron process freezes out, the AD field should have $B - L$ charge so that the sphaleron process does not wash out the asymmetry. In this section, we investigate the Affleck-Dine baryogenesis, taking into account the energy scale of inflation given in Eq. (1).

Since we assume that a flat direction obtains a large VEV in the early Universe, higher-dimensional terms should be taken into consideration. We assume an R-parity symmetry to avoid catastrophic proton decay, and superpotentials such as $W = \bar{u}\bar{d}\bar{d} \supset \phi^3$ disappears. Promoting this symmetry into a discrete R-symmetry which controls higher-dimensional terms for the flat direction, we assume the superpotential of the AD field as

$$W = \frac{\lambda\phi^n}{nM_{\text{pl}}^{n-3}}, \quad (6)$$

where M_{pl} ($\simeq 2.4 \times 10^{18}$ GeV) is the reduced Planck scale, λ is a coupling constant, and $n \geq 4$ is a certain integer which is determined by the R-charge of the AD field. For example, $n = 6, 9, 12, \dots$ for $\bar{u}d\bar{d}$ flat direction, depending on the discrete R-symmetry.

The AD field has usual soft terms as well as the F -term potential from the superpotential of Eq. (6) as

$$V_s = m_\phi (|\phi|)^2 |\phi|^2 + \left(\frac{-\lambda a_g}{n M_{\text{pl}}^{n-3}} m_{3/2} \phi^n + h.c. \right), \quad (7)$$

$$V_F = \frac{|\lambda|^2}{M_{\text{pl}}^{2n-6}} |\phi|^{2(n-1)}, \quad (8)$$

where $m_\phi(|\phi|)$ is the mass of the AD field at the energy scale of $|\phi|$. The term proportional to an $\mathcal{O}(1)$ parameter a_g is an A -term mediated by Planck-suppressed interactions, and $m_{3/2}$ is the mass of the gravitino. Hereafter, we set the phase of the AD field and the SUSY-breaking F -term such that $\text{Im}[\lambda] = 0$ and $\text{Im}[a_g] = 0$.

The AD field acquires Hubble induced terms during inflation [5], because inflation is associated with non-zero vacuum energy $V = 3H^2 M_{\text{pl}}^2$, which largely breaks SUSY. We write these Hubble-induced terms as

$$V_H = c_H H^2 |\phi|^2 + \left(\frac{-\lambda a_H}{n M_{\text{pl}}^{n-3}} H \phi^n + h.c. \right), \quad (9)$$

where c_H and a_H are $\mathcal{O}(1)$ constants. Hubble-induced A -terms are absent during inflation if the field which has a non-zero F -term during inflation is charged under some symmetry and its VEV is less than the Planck scale during inflation [9]. These conditions are usually satisfied for models of high-scale inflation in supergravity [44, 45] and thus we set $a_H = 0$ in this paper.³

As we show below, we have to take into account higher-dimensional terms V_K coming from a Kähler potential. Let us consider the following Kähler potential as an illustration for the origin of V_K :

$$K \sim I^\dagger I \frac{\phi^{n'}}{M_{\text{pl}}^{n'}}, \quad (10)$$

³ In models of D-term inflation [6–8], the Hubble-induced mass as well as the Hubble-induced A -term are absent: $c_H = a_H = 0$. However, the following discussion is also correct even if $c_H = 0$, due to the Hubble friction.

where I is a field which has a non-zero F -term during inflation (i.e. $|F_I|^2 = 3H^2 M_{\text{pl}}^2$). This operator gives the AD field a potential as

$$V_K = \left(\frac{-a_{H^2}}{n' M_{\text{pl}}^{n'-2}} H^2 \phi^{n'} + h.c. \right) + \dots, \quad (11)$$

where " \dots " denotes higher-dimensional Planck-suppressed terms. The parameter a_{H^2} is an $\mathcal{O}(1)$ constant.

To sum up, the potential of the AD field is given by the sum of the soft SUSY breaking terms V_s , the F -term potential V_F , the Hubble-induced terms V_H , and the potential coming from a Kähler potential V_K :

$$V = V_s + V_F + V_H + V_K. \quad (12)$$

In some cases, thermal potentials affect on the dynamics of the flat direction. As we see below, however, we are interested in the case that the VEV of the AD field is so large to evade the baryonic isocurvature constraint, which results in a low reheating temperature. Hence thermal potentials are irrelevant in the following discussion. In this paper, we set all unknown $\mathcal{O}(1)$ parameters as one: $|a_g|, |c_H|, |a_{H^2}| = 1$. We also assume $c_H < 0$, which makes the AD field obtain a large VEV during and after inflation as⁴

$$|\phi| \simeq \left(\frac{|c_H|}{(n-1)} \right)^{1/2(n-2)} \left(\frac{1}{\lambda} H M_{\text{pl}}^{n-3} \right)^{1/(n-2)}, \quad (13)$$

$$\simeq \begin{cases} 1 \times 10^{16} \text{ GeV} \lambda^{-1/2} \left(\frac{H}{10^{14} \text{ GeV}} \right)^{1/2} & \text{for } n = 4, \\ 2 \times 10^{17} \text{ GeV} \lambda^{-1/4} \left(\frac{H}{10^{14} \text{ GeV}} \right)^{1/4} & \text{for } n = 6, \\ 4 \times 10^{17} \text{ GeV} \lambda^{-1/6} \left(\frac{H}{10^{14} \text{ GeV}} \right)^{1/6} & \text{for } n = 8, \end{cases} \quad (14)$$

with the Hubble parameter being H_{inf} and $H(t)$, respectively. Note that if $\lambda = \mathcal{O}(10^{-4})$, the VEV of the AD field during inflation is as large as the Planck scale. Curvature of the phase direction of AD field, θ , is dominantly given by V_K ;

$$m_\theta^2 \equiv \frac{1}{2|\phi|^2} \frac{\partial^2 V}{\partial \theta^2}, \quad (15)$$

$$\simeq \frac{n'|a_{H^2}|}{2} H^2 \left(\frac{|\phi|}{M_{\text{pl}}} \right)^{n'-2}. \quad (16)$$

⁴ In the case of D-term inflation (i.e. $c_H = 0$), the AD field can stay anywhere $V'' \lesssim H$ is satisfied due to the Hubble friction. Eq. (14) is correct even in this case as long as the initial field value of the AD field is sufficiently large.

Note that the curvature is highly suppressed compared with H^2 for $|\phi| \lesssim M_{\text{pl}}$, that is, for $\lambda \gtrsim 10^{-4}$. (see Eqs. (1) and (14)).

After inflation ends, the energy density of the Universe is dominated by coherently oscillating inflaton and the Hubble parameter decreases as the Universe expands. When the Hubble-induced mass becomes less than the soft mass (i.e. $H(t) = H_{\text{osc}} \simeq m_\phi(\phi)$), the AD field begins to oscillate around the low-energy vacuum, $\phi = 0$. Since the phase of the AD field just before the oscillation begins is generally different from the one determined by the A -term of Eq. (7), the AD field also begins to rotate in the complex plane. Baryon number is generated by the rotation because baryon density is given by

$$n_B = -2b \text{Im} \left[\phi^* \dot{\phi} \right], \quad (17)$$

where b is the baryon charge of the AD field and the dot above the AD field denotes the derivative with respect to the time. For example, $b = -1/3$ for $\bar{u}d\bar{d}$ flat direction. The time evolution of the baryon density is written as

$$\dot{n}_B + 3Hn_B = 2b \text{Im} \left[\phi^* \frac{\partial V}{\partial \phi^*} \right]. \quad (18)$$

We estimate the solution of this equation as

$$\left(\frac{a(t)}{a(t_{\text{osc}})} \right)^3 n_B(t) = 2b \int a^3 \text{Im} \left[\phi^* \frac{\partial V}{\partial \phi^*} \right] dt, \quad (19)$$

$$\sim \lambda \frac{b}{H_{\text{osc}}} \frac{m_{3/2}}{M_{\text{pl}}^{n-3}} |\phi_{\text{osc}}|^n \sin(-n\theta), \quad (20)$$

$$\sim (b \sin(-n\theta)) m_{3/2} |\phi_{\text{osc}}|^2, \quad (21)$$

where θ is the initial phase of the AD field, which stays at a certain non-zero phase θ due to the Hubble friction before oscillation begins. We use $|\phi_{\text{osc}}|^n \sim H_{\text{osc}} |\phi_{\text{osc}}|^2 M_{\text{pl}}^{n-3}/\lambda$ in the last line. We define an ellipticity parameter as

$$\epsilon \equiv \frac{n_B/|b|}{n_\phi}, \quad (22)$$

$$\sim \text{sgn}(b) \sin(-n\theta) \frac{m_{3/2}}{H_{\text{osc}}}, \quad (23)$$

where $n_\phi \simeq \sqrt{V''} |\phi|^2$ is the number density of the AD field. In this paper, we assume $\epsilon = m_{3/2}/H_{\text{osc}}$, because the initial phase of the AD field θ is of the order of unity unless it is fine-tuned to coincide with the low energy vacuum $\theta = 0$. Thus we obtain the present

baryon-to-entropy ratio as

$$Y_B \equiv \frac{n_B}{s} = \frac{3T_{\text{RH}}}{4} \frac{n_B}{\rho_{\text{rad}}}\Big|_{\text{RH}} = \frac{3T_{\text{RH}}}{4} \frac{n_B}{\rho_{\text{inf}}}\Big|_{\text{RH}}, \quad (24)$$

$$= \frac{3T_{\text{RH}}}{4} \frac{n_B}{\rho_{\text{inf}}}\Big|_{\text{osc}} \simeq \frac{\epsilon |b| T_{\text{RH}}}{4H_{\text{osc}}} \left(\frac{|\phi_{\text{osc}}|}{M_{\text{pl}}} \right)^2, \quad (25)$$

where we use $\rho_{\text{inf}}|_{\text{osc}} \simeq 3M_{\text{pl}}^2 H_{\text{osc}}^2$ in the last line. Here we have assumed that there is no entropy production other than the decay of inflaton, which also implies that the AD field does not dominate the Universe. Note that if the AD field releases its charge into the standard model particles before the sphaleron process freezes out, there is an $\mathcal{O}(1)$ correction to Eq. (25) [46]. This is the case that we consider in Secs. V A and V C.

III. BARYONIC ISOCURVATURE PERTURBATION

Since there is no sizable Hubble-induced A-term, the phase direction of the AD field develops quantum fluctuations during inflation, and as a result a baryonic isocurvature fluctuation, which is tightly constrained by recent observations, is produced. In this section, we consider the dynamics of the phase direction of the AD field in detail.

First we consider the case of $\lambda \gg 10^{-4}$, in which the VEV of the AD field is so small that the potential V_K is negligible and the curvature of the phase direction is much less than the Hubble parameter during inflation (see Eq. (16)). The phase direction of the AD field therefore acquires quantum fluctuations during inflation as [6–9]

$$|\delta\theta| \simeq \frac{\sqrt{2}H_{\text{inf}}}{2\pi |\phi_{\text{inf}}|}. \quad (26)$$

Since the baryon number is related to the initial phase (see Eq. (21)), this fluctuation induces a sizable baryonic isocurvature fluctuation as

$$\mathcal{S}_{b\gamma} \equiv \frac{\delta Y_B}{Y_B} \simeq n \cot(n\theta) \delta\theta. \quad (27)$$

The baryonic isocurvature perturbation is constrained by observations of the cosmic microwave background, which have shown that the density perturbations are predominantly adiabatic [47, 48]. The *Planck* Collaboration puts an upper bound on the totally uncorrelated isocurvature fraction as [49]

$$\frac{\mathcal{P}_{SS}(k_*)}{\mathcal{P}_{\mathcal{RR}}(k_*) + \mathcal{P}_{SS}(k_*)} \lesssim 0.039, \quad (28)$$

where $\mathcal{P}_{\mathcal{RR}}$ and $\mathcal{P}_{\mathcal{SS}}$ are power spectra of the adiabatic fluctuation and isocurvature fluctuation, respectively, and k_* ($= 0.05 \text{ Mpc}^{-1}$) is a pivot scale. Since we are interested in the baryonic isocurvature fluctuation, we use the following relation:

$$\mathcal{P}_{\mathcal{SS}} = \left(\frac{\Omega_b}{\Omega_{\text{DM}}} \right)^2 \mathcal{P}_{\mathcal{S}_{b\gamma}\mathcal{S}_{b\gamma}}, \quad (29)$$

where Ω_b and Ω_{DM} are the density parameter of the baryon and DM, respectively. Thus we obtain an upper bound on the baryonic isocurvature fluctuation as

$$|\mathcal{S}_{b\gamma}| \lesssim \frac{\Omega_{\text{DM}}}{\Omega_b} (0.039 \times 2.2 \times 10^{-9})^{1/2} \simeq 5.0 \times 10^{-5}, \quad (30)$$

where we have used $\mathcal{P}_{\mathcal{RR}}^{1/2} \simeq 2.2 \times 10^{-9}$ [48]. The upper bound and the value of H_{inf} indicated by BICEP2 put a lower bound on ϕ_{inf} as

$$|\phi_{\text{inf}}| \gtrsim 4 \times 10^{17} \text{ GeV} \times n |\cot(n\theta)|. \quad (31)$$

This means that the VEV of the AD field should be as large as the Planck scale, which implies that the higher-dimensional operator in the superpotential should be suppressed, $\lambda \lesssim \mathcal{O}(10^{-4})$ (see Eq. (14)). When the AD field obtains such a large VEV, the potential V_K is effective and the phase direction of the AD field obtains a mass of the order of the Hubble parameter during inflation (see Eq. (16)).⁵ In this case, the baryonic isocurvature fluctuation is absent from the beginning. To summarize, in order to avoid a sizable baryonic isocurvature fluctuation, the VEV of the AD has to be as large as the Planck scale, in which case baryonic isocurvature fluctuation is absent due to the potential originated from a Kähler potential. Thus we assume $\lambda \lesssim 10^{-4}$ hereafter.⁶

Let us discuss the implication of the baryonic isocurvature fluctuation on the reheating temperature using Eq. (25). Since the VEV of the AD field at the beginning of its oscillation is related with that during inflation via $|\phi_{\text{osc}}| = (H_{\text{osc}}/H_{\text{inf}})^{1/(n-2)} |\phi_{\text{inf}}|$, a large VEV during inflation results in a relatively large VEV at the onset of its oscillation, and then the AD field tends to dominate the Universe. Therefore, in order to account for today's baryon-to-entropy ratio without additional entropy production except for the decay of inflaton, the reheating temperature tends to be small to dilute the AD field successfully.

⁵ In contrast, if $\lambda = \mathcal{O}(1)$, the lower bound in Eq. (31) requires about 1% and 10% tuning on the initial phase θ for $n = 4$ and $n = 6$ flat directions, respectively. This tuning would not be explained by the anthropic principle because human life would be able to exist whether or not baryonic isocurvature fluctuation exists. Taking this tuning seriously, we consider the case of $\lambda \lesssim 10^{-4}$ in this paper.

⁶ The smallness of λ might be understood by some flavor symmetry.

From Eq. (14), the VEV of the AD field at the beginning of its oscillation is given by

$$|\phi_{\text{osc}}| \simeq \begin{cases} 4 \times 10^{12} \text{ GeV} \left(\frac{\lambda}{10^{-4}}\right)^{-1/2} \left(\frac{H_{\text{osc}}}{1 \text{ TeV}}\right)^{1/2} & \text{for } n = 4, \\ 3 \times 10^{15} \text{ GeV} \left(\frac{\lambda}{10^{-4}}\right)^{-1/4} \left(\frac{H_{\text{osc}}}{1 \text{ TeV}}\right)^{1/4} & \text{for } n = 6, \\ 3 \times 10^{16} \text{ GeV} \left(\frac{\lambda}{10^{-4}}\right)^{-1/6} \left(\frac{H_{\text{osc}}}{1 \text{ TeV}}\right)^{1/6} & \text{for } n = 8, \end{cases} \quad (32)$$

where H_{osc} is the Hubble parameter at the oscillation time. Thus the observed baryon density requires the reheating temperature of the Universe as

$$T_{\text{RH}} \simeq \begin{cases} 4 \times 10^5 \text{ GeV} \epsilon^{-1} \left(\frac{\lambda}{10^{-4}}\right) & \text{for } n = 4, \\ 0.8 \text{ GeV} \epsilon^{-1} \left(\frac{\lambda}{10^{-4}}\right)^{1/2} \left(\frac{H_{\text{osc}}}{1 \text{ TeV}}\right)^{1/2} & \text{for } n = 6, \\ 9 \text{ MeV} \epsilon^{-1} \left(\frac{\lambda}{10^{-4}}\right)^{1/3} \left(\frac{H_{\text{osc}}}{1 \text{ TeV}}\right)^{2/3} & \text{for } n = 8, \end{cases} \quad (33)$$

where we have used $Y_B \simeq 8.7 \times 10^{-11}$ for the observed baryon-to-entropy ratio [50], and assumed $b = -1/3$. We should emphasize that the tight constraint on the baryonic isocurvature perturbation requires that $\lambda \lesssim 10^{-4}$ and puts a severe upper bound on the reheating temperature, if there is no additional entropy production. Eq. (33) is an important prediction from the BICEP2 result in a scenario for the Affleck-Dine baryogenesis. In Sec. V, we explain how the parameters ϵ and H_{osc} is determined for each scenario in gravity and gauge mediation.

Here we comment on the gauge symmetry breaking and its effect on the reheating process [51]. Since the non-zero VEV of the AD field breaks gauge symmetries, one may consider that the reheating process might be hindered. The hindrance of the reheating process occurs if the AD field continues to oscillate coherently and if the Standard Model gauge symmetry is completely broken by the VEV of the AD field. The former condition is not satisfied in the case that Q-balls are formed, which we explain in the next section. The latter condition is not satisfied for $\bar{u}d\bar{d}$ and LH_u flat directions, for example. As explained in Sec. V, Q-balls are usually formed in gauge mediation except for the case of LH_u flat direction. Thus, the suppression of the reheating process may be realized only in gravity mediation without Q-ball formation. This is the case we consider in Sec. V A, in which we check that the reheating process is not affected by the AD field at least in the case we are interested in (see Eq. (52)).

Finally, we comment on the case that the superpotential of the AD field is absent due to a discrete R-symmetry. In this case, the VEV of the AD field during inflation naturally becomes the Planck scale and thus a baryonic isocurvature fluctuation is absent. However,

the VEV at the beginning of its oscillation is also the Planck scale, at which the AD field still feels V_K . Since the potential of the AD field V_K is so complicated that the ellipticity parameter ϵ becomes $\mathcal{O}(1)$, Eq. (25) implies that the reheating temperature has to be much lower than 1 MeV in this case, which spoils the success of the BBN scenario. Thus we consider the case of $W \neq 0$.

IV. Q-BALLS

In this section, we explain the dynamics of the Q-ball, which is a non-topological soliton formed after the Affleck-Dine mechanism in many SUSY models [14–20]. We first explain the condition of the Q-ball to be formed and then review decay processes of the Q-ball.

A. Formation of Q-ball

After the AD field starts to oscillate and rotate around the low energy vacuum, the amplitude of the oscillation decreases due to the Hubble expansion. Since baryon number-violating terms are higher-dimensional ones, their effects become irrelevant and the generated baryon number is conserved soon after the beginning of the oscillation. Thus, in this section, we assume baryon number to be conserved and investigate the stable configuration of the AD field in a system with non-zero baryon charge.

The energy of the AD field is given as

$$E = \int d^3x \left[|\dot{\phi}|^2 + |\nabla\phi|^2 + V(|\phi|) \right]. \quad (34)$$

We are interested in the case with sufficiently small value of the AD field, for which the potential is approximated by $V = m_\phi^2(\phi) |\phi|^2$. Since the baryon density is already produced by the Affleck-Dine mechanism, we consider a system with non-zero baryon charge. The baryon charge is given by

$$Q = -2 \int d^3x \text{Im} \left[\phi^* \dot{\phi} \right], \quad (35)$$

where we have omitted the factor b for notational simplicity. The scalar field configuration which minimizes the energy given in Eq. (34) with a fixed baryon charge Q is obtained by minimizing the following combination;

$$E + \omega_0 \left[Q + 2 \int d^3x \text{Im} \left[\phi^* \dot{\phi} \right] \right], \quad (36)$$

where ω_0 is a Lagrange multiplier. Terms with time derivatives are rewritten as

$$|\dot{\phi}|^2 + 2\omega_0 \text{Im} [\phi^* \dot{\phi}] = \left| \dot{\phi} + i\omega_0 \phi \right|^2 - \omega_0^2 |\phi|^2. \quad (37)$$

The minimization condition determines the time dependence of the AD field as

$$\phi(\mathbf{r}, t) = \varphi(\mathbf{r}) e^{-i\omega_0 t} / \sqrt{2}. \quad (38)$$

Assuming a spherically symmetric ansatz, $\varphi(\mathbf{r}) = \varphi(r)$, we obtain the following equation which determines $\varphi(r)$:

$$\frac{\partial^2}{\partial r^2} \varphi + \frac{2}{r} \frac{\partial}{\partial r} \varphi + \omega_0^2 \varphi - \frac{\partial}{\partial \varphi} V(\varphi) = 0. \quad (39)$$

The boundary condition is $\varphi'(0) = 0$ and $\varphi(\infty) = 0$ since we are interested in smooth and localized configurations. Regarding ϕ and r as a position and a time variable, Eq. (39) is interpreted as the equation of motion of a particle in one dimension with a friction term $(2/r)\partial\varphi/\partial r$. Using this analogy, one can find the following condition for existence of a spatially localized configuration, referred to as Q-ball [20]:

$$\min_{\varphi} \left[\frac{2V(\varphi)}{\varphi^2} \right] < \omega_0^2 < \frac{\partial^2 V(0)}{\partial \varphi^2}. \quad (40)$$

In most cases we are interested in, the energy of the Q-ball per unit charge is well approximated by ω_0 .

Linear analyses indicate that there are instability bands during the oscillation of the AD field which corresponds to a typical size of the Q-ball R if the condition of Q-ball formation Eq. (40) is satisfied [15, 16]. This means that the coherently oscillating AD field is unstable and fragments into Q-balls soon after the onset of its oscillation. A typical charge of Q-balls is roughly estimated by the charge which is contained in the volume of a typical Q-ball size R at the formation time:

$$Q \sim n_B(t_{form}) R^3 \sim \left(\frac{a(t_{osc})}{a(t_{form})} \right)^3 \omega_0 |\phi_{osc}|^2 R^3, \quad (41)$$

where we have included the dependence on the scale factors a because it needs some time for Q-ball to be formed completely. The numerical simulations have shown that Q-balls are indeed formed when the condition of Q-ball formation Eq. (40) is satisfied, and have determined the proportional constant including $a^3(t_{osc})/a^3(t_{form})$ of Eq. (41) for the cases we are interested in (see Eqs. (79) and (117)) [17–19, 52].

B. Decay of Q-ball

To explain the decay of Q-balls, let us focus on a Q-ball which consists only of squarks. Numerical simulations have shown that almost all of the baryon charge of the AD field are transferred into Q-balls [17–19, 52]. Then Q-balls decay and release their baryon charge into quarks if they are unstable. The AD field interacts with quarks via gauge interactions and thus Q-balls lose their baryon charge by emitting quarks from their surfaces [21].⁷ The condition for Q-ball decay is that the energy of the Q-ball per unit baryon charge, $\omega_0/|b|$, is larger than masses of baryons in the hadron phase, $m_b \simeq 1 \text{ GeV}$.

Usually, the baryon charge density inside a Q-ball is so large that a naive rate estimated by squark decay exceeds an upper limit by the Pauli blocking effect. The rate of particle emission from a Q-ball surface is therefore determined by the Pauli blocking effect on its surface and is given as [21]⁸

$$\frac{dN}{dt} \simeq \sum_i 4\pi \tilde{R}^2 \mathbf{n} \cdot \mathbf{j}_i, \quad (42)$$

$$\begin{aligned} \mathbf{n} \cdot \mathbf{j}_i &\simeq 2 \int \frac{d^3k}{(2\pi)^3} \theta(E_i/2 - |\mathbf{k}|) \theta(\mathbf{k} \cdot \mathbf{n}) \hat{\mathbf{k}} \cdot \mathbf{n} \\ &= \frac{E_i^3}{96\pi^2}, \end{aligned} \quad (43)$$

where \mathbf{n} is the outward-pointing normal vector, \mathbf{j} is particle flux, and \tilde{R} is the effective radius of the Q-ball given by $\phi(\tilde{R}) \sim \omega_0$ [53]. The interaction energy E_i is given by the energy of the Q-ball per unit charge, ω_0 , when the relevant elementary process is squark decay, such as $\tilde{q} \rightarrow q + (\text{gaugino})$. In addition, the baryon charge density inside the Q-ball is so large that the scattering process via gaugino (or Higgsino) exchange $\tilde{q} + \tilde{q} \rightarrow q + q$ occurs efficiently. It has been shown that the rate of this process is also saturated by the Pauli blocking effect, and the interaction energy E_i is given by $2\omega_0$ in this case [53]. The rate of Q-ball decay is dominated by the latter process and thus its lifetime Γ_Q^{-1} is given as

$$\Gamma_Q^{-1} \simeq \left(\frac{1}{Q} \frac{dN}{dt} \right)^{-1}, \quad (44)$$

$$\simeq \left(8n_q \frac{\tilde{R}^2 \omega_0^3}{24\pi Q} \right)^{-1}, \quad (45)$$

⁷ Far inside Q-balls, field values of squarks are large and hence gauginos and quarks are heavy. Therefore, Q-balls cannot decay into them.

⁸ Here we assume that quarks and gauginos are massless. A correction for the flux of massive particles is derived in the Appendix.

where n_q is the number of species for quarks interacting with the AD field and is typically $\mathcal{O}(10)$.

Q-balls completely lose their charge and energy when the condition $\Gamma_Q \sim H$ is satisfied. The decay temperature of Q-ball is thus determined as

$$T_{\text{decay}} \simeq \begin{cases} T_{\text{RH}} \left(\sqrt{\frac{30}{\pi^2 g_*}} \frac{\Gamma_Q M_{\text{pl}}}{T_{\text{RH}}^2} \right)^{1/4} & \text{for } T_{\text{decay}} > T_{\text{RH}}, \\ \left(\frac{90}{4\pi^2 g_*} \right)^{1/4} \sqrt{\Gamma_Q M_{\text{pl}}} & \text{for } T_{\text{decay}} < T_{\text{RH}}, \end{cases} \quad (46)$$

where the first line is the case where Q-balls decay before reheating completes while the second one is the case where Q-balls decay after reheating completes. In the latter case, the energy density of Q-balls may dominate the Universe. Since Q-balls are localized lumps much smaller than the horizon scale, their energy density decreases as a^{-3} , where a is a scale factor. Thus the energy density of Q-balls dominates that of the Universe when the following condition is satisfied:

$$1 \lesssim \frac{\rho_Q}{\rho_r} \Big|_{T=T_{\text{decay}}} \simeq \frac{\rho_Q}{\rho_r} \Big|_{T=T_{\text{RH}}} \left(\frac{T_{\text{RH}}}{T_{\text{decay}}} \right), \quad (47)$$

$$\simeq \frac{\rho_\phi}{\rho_I} \Big|_{\text{osc}} \left(\frac{T_{\text{RH}}}{T_{\text{decay}}} \right) \simeq \frac{\phi_{\text{osc}}^2}{3M_{\text{pl}}^2} \left(\frac{T_{\text{RH}}}{T_{\text{decay}}} \right), \quad (48)$$

where ρ_I is the inflaton energy. We checked that the energy density of Q-balls never dominate that of the Universe in the case we consider.

As explained above, Q-balls dominantly decay into quarks. However, they decay into SUSY particles if the decay process is kinematically allowed. From kinematics and the conservation of baryon charge, Q-ball can decay only into particles lighter than the energy of the Q-ball per unit charge, ω_0 . Since ω_0 is less than the mass of the AD field (see Eq. (40)), Q-balls cannot decay into the AD field itself. This is another explanation of the stability of Q-ball. On the other hand, Q-balls decay into gauginos and/or Higgsinos if they interact with the Q-balls and their masses are less than ω_0 . However, in contrast to the case of quarks, gauginos and Higgsinos cannot be produced through a scattering process like $\tilde{q} + \tilde{q} \rightarrow (\text{gaugino}) + (\text{gaugino})$ due to the conservation of baryon charge. Thus if we could neglect their masses, their production rate from Q-ball decay is given by Eq. (43) with $E_i = \omega_0$. In addition, there is a correction coming from non-zero masses of gauginos and Higgsinos as explained in the Appendix.

V. SCENARIOS FOR DARK MATTER PRODUCTION IN LOW REHEATING TEMPERATURE

To construct a consistent cosmological scenario, it is necessary to account for the following observed DM density as well as the baryon density:

$$\frac{\rho_{\text{DM}}}{s} \simeq (3.5 \text{ eV}) \times \Omega_{\text{DM}} h^2, \quad (49)$$

$$\simeq 0.44 \text{ eV}, \quad (50)$$

where we have used $\Omega_{\text{DM}} h^2 \simeq 0.12$ for the observed DM abundance in the last line [50]. As explained in Sec. III, the reheating temperature of the Universe must satisfy Eq. (33) to account for the observed baryon density by the Affleck-Dine baryogenesis. In this section, we propose scenarios to account for the DM density in that reheating temperature.

Assuming models of gravity mediation and gauge mediation, we investigate scenarios in each model with and without Q-ball formation. In Sec. V A, we consider a model of gravity mediation without Q-ball formation, in which DM is mainly produced from two processes; decay and inelastic scatterings during reheating era [33, 34]. In Sec. V B, we consider a model of gravity mediation with Q-ball formation. In this case, DM can be produced from Q-balls [16, 22–26, 32] as well as by the above two processes. In Sec. V C, we consider a model of gauge mediation without Q-ball formation, which is only the case for LH_u flat direction. In this case, gravitino DM is produced from the thermal plasma at the time of reheating [40] as well as from decay and inelastic scatterings during reheating era. A model of gauge mediation with Q-ball formation is investigated in Sec. V D. Also in this case, Q-balls provide another source of DM [27–31].

A. Gravity mediation without Q-ball

In models of gravity mediation, the mass of the AD field $m_\phi(|\phi|)$ logarithmically depends on $|\phi|$ due to renormalization group running of squark masses, and the condition for Q-ball formation, Eq. (40), is satisfied when the mass decreases with increasing the VEV of the AD field (i.e. $dm_\phi/d\phi < 0$) [16]. While the strong interaction makes squarks light with increasing energy scale, Yukawa interactions make them heavy. In a typical model of gravity mediation, stops become heavy with increasing energy scale while the first and second family squarks become light. Thus there may be no Q-ball solution if the AD field consists mainly

of third family squarks. In this subsection, we consider the case without Q-ball formation in gravity mediation.

Since gravitino mass is of the same order as squark masses in gravity mediation, the ellipticity parameter, ϵ ($= m_{3/2}/H_{\text{osc}} \simeq m_{3/2}/m_\phi(\phi_{\text{osc}})$), is of the order of one (see Eq. (23)). Thus we obtain the VEV of the AD field at the beginning of its oscillation and the reheating temperature of the Universe from Eqs. (32) and (33). Assuming that the AD field continues to oscillate until reheating completes, we calculate the amplitude of the oscillation at the time of reheating as

$$\begin{aligned} \phi|_{T=T_{\text{RH}}} &\simeq \phi_{\text{osc}} \frac{T_{\text{RH}}^2}{H_{\text{osc}} M_{\text{pl}}}, & (51) \\ &\simeq \begin{cases} 3 \times 10^2 \text{ GeV} \left(\frac{\lambda}{10^{-4}}\right)^{3/2} \left(\frac{H_{\text{osc}}}{1 \text{ TeV}}\right)^{-1/2} & \text{for } n = 4, \\ 7 \times 10^{-7} \text{ GeV} \left(\frac{\lambda}{10^{-4}}\right)^{3/4} \left(\frac{H_{\text{osc}}}{1 \text{ TeV}}\right)^{1/4} & \text{for } n = 6, \\ 9 \times 10^{-10} \text{ GeV} \left(\frac{\lambda}{10^{-4}}\right)^{1/2} \left(\frac{H_{\text{osc}}}{1 \text{ TeV}}\right)^{1/2} & \text{for } n = 8. \end{cases} & (52) \end{aligned}$$

Thus we find that the amplitude of the oscillation at the time of reheating is much less than the reheating temperature. This indicates that the AD field cannot affect the reheating process even if it could continue to oscillate coherently. Of course, the coherent oscillation dissipates through interactions with the thermal plasma much before reheating completes, but in this paper we do not investigate this issue in detail (see Ref. [51, 55] and references therein).

The Affleck-Dine baryogenesis with $n = 4$ flat direction predicts the reheating temperature as $T_{\text{RH}} \simeq 4 \times 10^5 \text{ GeV}$ for $\lambda = 10^{-4}$, in which case DM is produced thermally. Since the LSP is mostly bino-like in a typical model of gravity mediation, thermally produced binos over-closes the Universe unless the mass of bino is fine-tuned to co-annihilate [56, 57] with the stau [58]. On the other hand, when we consider $n = 4$ flat direction with $\lambda \lesssim 10^{-10}$ or $n = 6, 8$ flat direction with $\lambda \lesssim 10^{-4}$, the required reheating temperature is less than 1 GeV (see Eq. (33)). Such a low reheating temperature results in a non-thermal production of DM, which we have investigated in Ref. [33]. Here we review this calculation and apply it in our situation. In a low reheating temperature, DM is produced mainly through two contributions: direct decay of inflaton into SUSY particles [34–39] and inelastic scatterings between high energy particles and thermal plasma during reheating process [33, 34].⁹

⁹ DM is also produced thermally if the maximal temperature of the Universe is larger than the freeze-out temperature of the LSP [54, 59]. However, this contribution is always subdominant as shown in Ref. [33], and we neglect it in this paper.

DM can be produced directly by the decay of inflaton [35–39] and its abundance is calculated as

$$\frac{\rho_{\text{DM}}^{\text{dir}}}{s} \simeq m_{\text{DM}} \frac{3T_{\text{RH}} n_{\text{DM}}}{4\rho_I} \Big|_{T=T_{\text{RH}}}, \quad (53)$$

$$\simeq m_{\text{DM}} \frac{3T_{\text{RH}}}{4m_I} \text{Br}_I, \quad (54)$$

$$\simeq 0.4 \text{ eV} \left(\frac{m_{\text{DM}}}{1 \text{ TeV}} \right) \left(\frac{T_{\text{RH}}}{0.1 \text{ GeV}} \right) \left(\frac{m_I}{10^{12} \text{ GeV}} \right)^{-1} \left(\frac{\text{Br}_I}{5} \right), \quad (55)$$

where m_{DM} is the mass of the LSP, and m_I is the mass of the inflaton. We write Br_I as the average number of DM produced by each inflaton decay. One may expect $\text{Br}_I = 1$ due to SUSY. In Ref. [39], however, it was pointed out that SUSY particles are produced through a cascade shower from inflaton decay, like pions in a QCD shower, and the effective branching ratio Br_I deviates from 1. They calculated Br_I and found that Br_I is as large as $\mathcal{O}(10^{0-1})$ for $m_I = 10^{10}$ GeV. They also extrapolated the results from $m_I \leq 10^{10}$ GeV to larger inflaton mass and estimated $\text{Br}_I = \mathcal{O}(10^{0-2})$ for $m_I = 10^{13}$ GeV.

Next, let us explain the other process of DM production; inelastic scattering process during the reheating era [33, 34]. At the first stage of reheating, the inflaton decays into high energy particles with the energy of the order of the inflaton mass m_I . The daughter particles interact with each other and produce many low energy particles almost without losing their energy. Then low energy particles thermalize by their own interactions, but the energy of the thermal plasma is still much smaller than that of the inflaton. Once the thermal plasma is created in the Universe, the high energy particles produced from the inflaton decay inelastically interact with the thermal plasma, through which the number of high energy particles drastically increases [60, 61] (see also Ref. [62–64]). Throughout this process, DM is produced in a certain amount as we explain below.¹⁰

Let us estimate an inelastic scattering cross section between a high energy particle and the thermal bath. It is enhanced by t -channel contribution and is given as

$$\sigma_{\text{inelastic}} \sim \frac{\alpha^3}{t} \sim \frac{\alpha^2}{T^2}, \quad (56)$$

where an infrared divergence is naturally regulated by the thermal mass of an internal field, $\alpha^{1/2}T$. However, in estimating the scattering rate, it is necessary to take into account

¹⁰ The following estimation of the DM abundance involves uncertainties. For example, the estimation of the rate of inelastic scatterings is based on qualitative discussions. Therefore, the prediction on the DM mass given below has an uncertainty within about one order of magnitude.

an interference effect between a daughter particle and its parent particle, known as the Landau-Pomeranchuk-Migdal (LPM) effect [65–71]. The interference effect forbids subsequent scattering processes while their phase spaces overlap with each other. When we write the position vector of a parent particle as $x^\mu = (\Delta t, \Delta t \hat{z})$, the interference effect remains until the phase factor varies significantly as

$$1 \lesssim kx \sim \Delta t k^0 \theta^2 \sim \Delta t k_\perp^2 / k^0, \quad (57)$$

where k and k_\perp are the four momentum and the perpendicular momentum of the daughter particle, respectively.¹¹ We write the emission angle of the daughter particle as $\theta (= k_\perp / k^0)$. From Eq. (57), we find that the LPM effect suppresses subsequent inelastic scattering processes during the interval $\Delta t(k^0) \sim k^0 / k_\perp^2$. We therefore determine the inelastic scattering rate as

$$\Gamma_{\text{inelastic}} \sim \min \left[\langle \sigma_{\text{inelastic}} n \rangle, \int \frac{dk^0}{k^0} \frac{\alpha}{\Delta t(k^0)}, \right]. \quad (58)$$

Let us estimate the perpendicular momentum of the daughter particle Δk_\perp . The perpendicular momentum evolves as random walk due to elastic scatterings with the thermal plasma as

$$(\Delta k_\perp)^2 \sim \hat{q}_{\text{el}} t, \quad (59)$$

where \hat{q}_{el} is a diffusion constant given by the elastic scattering rate $\Gamma_{\text{el}} (\simeq \alpha T)$ as

$$\hat{q}_{\text{el}} \sim \int d^2 q_\perp \frac{\partial \Gamma_{\text{el}}}{\partial q_\perp^2} q_\perp^2 \sim \alpha^2 T^3. \quad (60)$$

Using Eqs. (59) and (60), we obtain

$$\Delta t \sim \left(\frac{k^0}{\hat{q}_{\text{el}}} \right)^{1/2} \sim \frac{1}{\alpha T} \left(\frac{k^0}{T} \right)^{1/2}. \quad (61)$$

The rate of inelastic scatterings is determined by Eqs. (58) and (61), from which we find that the energy loss rate increases with increasing the energy of the daughter particle. Therefore high energy particles from the inflaton decay continue to split into high energy particles whose energy is less than but the same in order of magnitude as parent particle's energy. Throughout this splitting process, the number density of high energy particles

¹¹ Here and hereafter we assume that the daughter particle is charged under a non-Abelian gauge group.

increases exponentially [60, 61]. Given a certain time when their energy is of the order of E , we can estimate their number density n_h from the energy conservation as

$$n_h \sim \frac{m_{\text{I}}}{E} n_{\text{I}}, \quad (62)$$

where n_{I} is the number density of the inflaton [33].

During the above splitting process, inelastic scatterings between a high energy particle and the thermal plasma can produce DM, when the center-of-mass energy $\sqrt{4TE}$ is larger than the mass of DM m_{DM} . The production rate is given as [34]

$$\Gamma_{\text{DM}} \sim \langle \sigma_{\text{DM}} n_r \rangle \sim \frac{\alpha^2 T^3}{m_{\text{DM}}^2}, \quad (63)$$

for a reaction whose center-of-mass energy is just above the threshold (i.e. $E \gtrsim E_{\text{th}} \equiv m_{\text{DM}}^2/4T$). Although the fine structure constant α for the DM production process is in general different from the one for the inelastic scattering process, we neglect the difference in this paper for simplicity. The energy density of DM which is produced during the splitting process of high energy particles is therefore obtained as

$$\frac{\rho_{\text{DM}}^{\text{inela}}}{s} \sim m_{\text{DM}} \frac{\Gamma_{\text{DM}}}{\Gamma_{\text{inelastic}}} \frac{n_h}{s}, \quad (64)$$

$$\sim m_{\text{DM}} \frac{\alpha^2 T_{\text{RH}}^3}{m_{\text{DM}}^2} \frac{\sqrt{E_{\text{th}}}}{\alpha^2 T_{\text{RH}} \sqrt{T_{\text{RH}}}} \frac{m_{\text{I}}}{E_{\text{th}}} \frac{n_{\text{I}}}{s} \quad (65)$$

$$\sim \frac{T_{\text{RH}}^3}{m_{\text{DM}}^2}, \quad (66)$$

$$\sim 1 \text{ eV} \left(\frac{T_{\text{RH}}}{0.1 \text{ GeV}} \right)^3 \left(\frac{m_{\text{DM}}}{1 \text{ TeV}} \right)^{-2}. \quad (67)$$

Note that the DM abundance is independent of the mass of the inflaton. In general, the gauge coupling constants in the second line cannot be canceled with each other, but our conclusion is still correct with an uncertainty within one order of magnitude.

Here we comment on some assumptions which we have implicitly used in the above calculation. We assume that the inflaton is so heavy that its daughter particles can produce DM at the time of $T = T_{\text{RH}}$ (i.e. $m_{\text{I}} \geq m_{\text{DM}}^2/2T_{\text{RH}} \sim 10^7 \text{ GeV}$). Since the energy scale of inflation is large, it is expected that the inflaton mass is also large. The other case has been calculated in the original paper [33]. In addition, the result in Eq. (67) is over-estimated for the reheating temperature smaller than the QCD scale ($\sim 0.1 \text{ GeV}$), because some hadrons, such as neutral pion, have no gauge interactions and the energy loss by splitting processes may be suppressed.

Finally, let us consider the annihilation of DM. The DM abundance is reduced by its annihilation if $\langle\sigma_{\text{ann}}v\rangle n_{\text{DM}} \gtrsim H_{T=T_{\text{RH}}}$, where $\langle\sigma_{\text{ann}}v\rangle$ is the thermally averaged annihilation cross section of DM. This implies that there is an upper bound on the DM abundance given as

$$\begin{aligned} \frac{\rho_{\text{DM}}^{\text{ann}}}{s} &\simeq \sqrt{\frac{45}{8\pi^2 g_*}} \frac{m_{\text{DM}}}{T_{\text{RH}} \langle\sigma_{\text{ann}}v\rangle M_{\text{pl}}}, \\ &\simeq 0.9 \text{ eV} \left(\frac{T_{\text{RH}}}{1 \text{ GeV}}\right)^{-1} \left(\frac{m_{\text{DM}}}{1 \text{ TeV}}\right) \left(\frac{\langle\sigma_{\text{ann}}v\rangle}{0.1 \text{ TeV}^{-2}}\right)^{-1}. \end{aligned} \quad (68)$$

The LSP is mostly bino-like in a typical model of gravity mediation. Its annihilation effect is negligible as far as its abundance is consistent with the observed DM abundance.

In summary, DM can be produced from two sources, and its abundance is given by the sum of Eqs. (55) and (67). Taking the annihilation of DM into account, we conclude that the DM abundance is given by

$$\frac{\rho_{\text{DM}}}{s} \simeq \min \left[\frac{\rho_{\text{DM}}^{\text{dir}}}{s} + \frac{\rho_{\text{DM}}^{\text{inela}}}{s}, \frac{\rho_{\text{DM}}^{\text{ann}}}{s} \right]. \quad (69)$$

In Fig. 1, we show the constraint on the DM mass m_{DM} and the reheating temperature T_{RH} . The left and the right panels assume the inflaton mass m_ϕ of 10^{13} GeV and 10^{15} GeV, respectively.¹² On the boundary of and inside the red (light gray) shaded region, the decay of the inflaton produces DM density equal to and larger than the observed one. On the boundary and inside the blue (dark gray) shaded region, inelastic scatterings during the thermalization process produce the correct and larger amount of DM. As we have mentioned, for $T_{\text{RH}} \lesssim 0.1$ GeV, the thermalization process involves scatterings of hadrons and the DM abundance produced by inelastic scatterings may be over-estimated. We also show the requirement of the reheating temperature from the successful Affleck-Dine Baryogenesis. The green-dashed, red-dotted, and blue lines show the required reheating temperature for $n = 4$ with $\lambda = 10^{-10}$, $n = 6$ with $\lambda = 10^{-6}$, and $n = 8$ with $\lambda = 10^{-4}$, respectively.

From Fig. 1, we predict the mass of DM as

$$m_{\text{DM}} \simeq \begin{cases} 3 \text{ TeV} \left(\frac{m_I}{10^{12} \text{ GeV}}\right) \left(\frac{\text{Br}_I}{5}\right)^{-1} \left(\frac{\lambda}{10^{-11}}\right)^{-1}, & \text{for } n = 4, \\ 0.7 \text{ TeV} \left(\frac{m_I}{10^{13} \text{ GeV}}\right) \left(\frac{\text{Br}_I}{5}\right)^{-1} \left(\frac{\lambda}{10^{-4}}\right)^{-1/2} \left(\frac{H_{\text{osc}}}{5 \text{ TeV}}\right)^{-1/2}, & \text{for } n = 6 \\ 0.4 \text{ TeV} \left(\frac{m_I}{10^{11} \text{ GeV}}\right) \left(\frac{\text{Br}_I}{5}\right)^{-1} \left(\frac{\lambda}{10^{-4}}\right)^{-1/3} \left(\frac{H_{\text{osc}}}{5 \text{ TeV}}\right)^{-2/3}, & \text{for } n = 8, \end{cases} \quad (70)$$

¹² In large field models discussed in Refs. [72, 73], the inflaton mass can be as large as 10^{15} GeV.

or

$$m_{\text{DM}} \simeq \begin{cases} 0.4 \text{ TeV} \left(\frac{\lambda}{10^{-11}}\right)^{3/2}, & \text{for } n = 4, \\ 3 \text{ TeV} \left(\frac{\lambda}{10^{-6}}\right)^{3/4} \left(\frac{H_{\text{osc}}}{5 \text{ TeV}}\right)^{3/4}, & \text{for } n = 6, \\ 0.2 \text{ TeV} \left(\frac{\lambda}{10^{-4}}\right)^{1/2} \left(\frac{H_{\text{osc}}}{5 \text{ TeV}}\right), & \text{for } n = 8, \end{cases} \quad (71)$$

where we assume $\epsilon = 1$. Eq. (70) is the case where the DM abundance is determined by the contribution from the decay of inflaton, while Eq. (71) is the case where the DM abundance is determined by the contribution from inelastic scattering process during reheating.¹³ Note that H_{osc} is roughly given by the squark mass at the energy scale $\phi_{\text{osc}} \sim 10^{15}$ GeV, and the parameter λ has an upper bound as $\lambda \lesssim 10^{-4}$ to avoid a sizable baryonic isocurvature perturbation as explained in Sec. II.

Interestingly, by combining Eqs. (55) and (67), we obtain a lower bound on the inflaton mass as a function of reheating temperature as

$$m_I \gtrsim 1.3 \times 10^{12} \text{ GeV} \left(\frac{\text{Br}_I}{5}\right) \left(\frac{T_{\text{RH}}}{0.1 \text{ GeV}}\right)^{5/2}, \quad (72)$$

to obtain the correct DM density, Eq. (50). Although we can evade this constraint for $T_{\text{RH}} \gtrsim m_{\text{DM}}$, only $n = 4$ flat direction with $\lambda \gg 10^{-10}$ is consistent with such a high reheating temperature. Otherwise, the DM abundance exceeds the observed one whatever the DM mass is.

Finally, we comment on the testability of this scenario. For SUSY particles with masses of $\mathcal{O}(1)$ TeV, the elastic scattering cross section between the bino-like LSP and nucleon is as large as $10^{-46} - 10^{-45} \text{ cm}^2$, which is detectable in future direct detection experiments of DM such as XENON1T [74]. Since the thermal relic of the bino-like LSP is usually much larger than the observed DM abundance, the above scenario would be favored if DM is detected in that region.

B. Gravity mediation with Q-balls

As we have mentioned in the previous subsection, the mass of the AD field $m_\phi(|\phi|)$ logarithmically depends on $|\phi|$ due to the renormalization group running of squark masses.

¹³ As we have mentioned, the prediction given in Eq. (71) involves an uncertainty within about one order of magnitude.

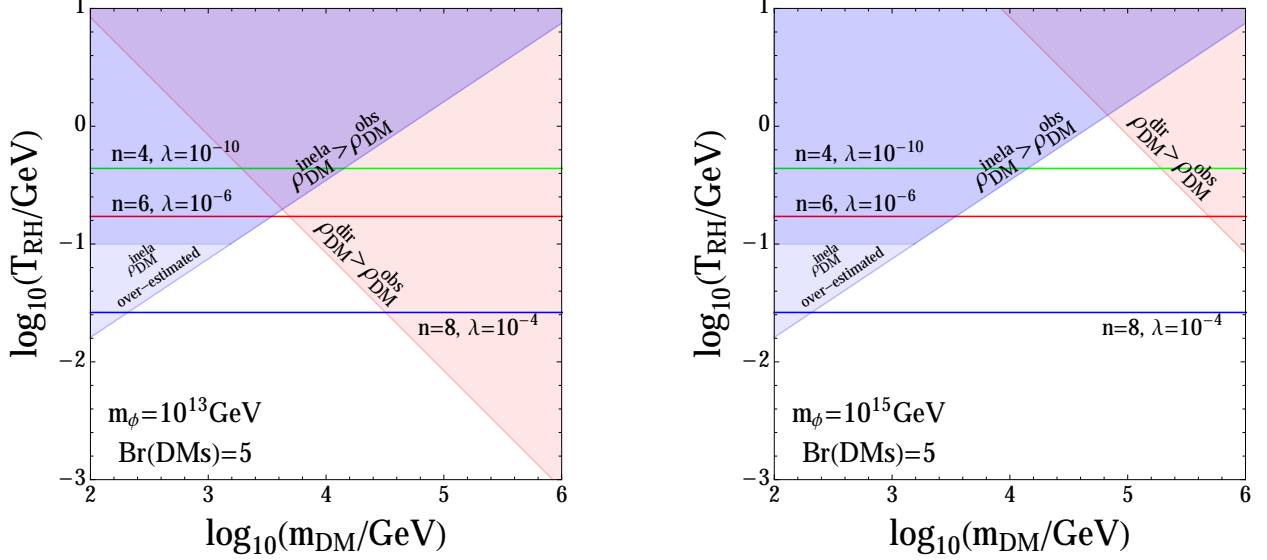


FIG. 1. Exclusion plot in a model of gravity mediation without Q-ball formation. We assume that the effective branching of inflaton decay into DM is 5 and the mass of the inflaton m_I is 10^{13} GeV (left panel) and 10^{15} GeV (right panel). The abundance of DM produced from direct decay of inflaton ($\rho_{\text{DM}}^{\text{dir}}$) and inelastic scatterings ($\rho_{\text{DM}}^{\text{inela}}$) is larger than that observed in the red (light gray) and blue (dark gray) shaded region, respectively. The blue (dark gray) shaded region with a temperature lower than 0.1 GeV is the region in which $\rho_{\text{DM}}^{\text{inela}}$ is over-estimated. The horizontal green-dashed, red-dotted, and blue lines are the reheating temperature required by the success of the Affleck-Dine baryogenesis for $n = 4$ with $\lambda = 10^{-10}$, $n = 6$ with $\lambda = 10^{-6}$, and $n = 8$ with $\lambda = 10^{-4}$, respectively. We take $H_{\text{osc}} = 5$ TeV.

We basically write the potential of the AD field in gravity mediation as

$$V = m_\phi^2(|\phi|)|\phi|^2 = m_\phi^2|\phi|^2 \left(1 + K \log \frac{|\phi|^2}{M_{\text{pl}}^2} \right), \quad (73)$$

where the second term in the parenthesis represents renormalization group running. In many cases in gravity mediation, the strong interaction dominates quantum corrections for a typical flat direction, and we obtain $K < 0$ and $|K| \sim 0.01 - 0.1$ [16], which satisfies the condition for Q-ball formation in Eq. (40). The configuration of the AD field is obtained by solving Eq. (39) with the above potential. The solution is well approximated by [16]

$$\phi(r, t) \simeq \frac{1}{\sqrt{2}} \phi_0 e^{-r^2/2R^2} e^{-i\omega_0 t}, \quad (74)$$

where R , ω_0 , and ϕ_0 are given as

$$R \simeq \frac{1}{|K|^{1/2} m_\phi(\phi_0)}, \quad (75)$$

$$\omega_0 \simeq m_\phi(\phi_0), \quad (76)$$

$$\phi_0 \simeq \left(\frac{|K|}{\pi} \right)^{3/4} m_\phi(\phi_0) Q^{1/2}, \quad (77)$$

where $m_\phi(\phi_0)$ is the mass of the AD field at the energy scale of ϕ_0 . Since the energy of the Q-ball, M_Q , is calculated from Eq. (34) as

$$M_Q \simeq m_\phi(\phi_0) Q, \quad (78)$$

we find that the energy of the Q-ball per unit charge is approximately equal to $\omega_0 \simeq m_\phi \gg 1$ GeV and thus Q-balls decay into quarks.

Using $\omega_0 \simeq m_\phi$ and $R \sim m_\phi^{-1}$ in Eq. (41), we estimate a typical charge of Q-ball formed after the Affleck-Dine baryogenesis as

$$Q \sim \beta \left(\frac{|\phi_{\text{osc}}|}{m_\phi} \right)^2, \quad (79)$$

$$\simeq 2 \times 10^{23} \left(\frac{|\phi_{\text{osc}}|}{3 \times 10^{15} \text{ GeV}} \right)^2 \left(\frac{m_\phi}{1 \text{ TeV}} \right)^{-2}. \quad (80)$$

The numerical simulations have shown that the coefficient β is approximately given by 2×10^{-2} [17, 18, 52], which we have used in the second line.

The decay rate of the Q-ball is calculated from Eq. (45) with $\tilde{R} \simeq R(2 \log(\phi_0/\sqrt{2}\omega_0))^{1/2} \simeq 7R$. For $n = 4$, the Q-ball decays after the reheating as

$$T_{\text{decay}} \simeq 10^3 \text{ GeV} \left(\frac{\lambda}{10^{-4}} \right)^{1/2} \left(\frac{H_{\text{osc}}}{1 \text{ TeV}} \right)^{-1/2} \left(\frac{m_\phi}{1 \text{ TeV}} \right)^{3/2}, \quad \text{for } n = 4, \quad (81)$$

where we assume that the effective number of relativistic degrees of freedom at the decay time g_* is about 200, and $n_q \sim 10$. Using Eq. (48), we checked that the energy density of Q-balls never dominates the Universe. For $n = 6$ and $n = 8$, the Q-ball decays just before the reheating as

$$T_{\text{decay}} \simeq \begin{cases} 2 \text{ GeV} \left(\frac{\lambda}{10^{-4}} \right)^{3/8} \left(\frac{H_{\text{osc}}}{1 \text{ TeV}} \right)^{1/8} \left(\frac{m_\phi}{1 \text{ TeV}} \right)^{3/4}, & \text{for } n = 6, \\ 60 \text{ MeV} \left(\frac{\lambda}{10^{-4}} \right)^{1/4} \left(\frac{H_{\text{osc}}}{1 \text{ TeV}} \right)^{1/4} \left(\frac{m_\phi}{1 \text{ TeV}} \right)^{3/4}, & \text{for } n = 8, \end{cases} \quad (82)$$

where we assume that the effective number of relativistic degrees of freedom at the decay time g_* is 10.75. We find that Q-balls decay after DM freezes out for $n = 6$ and $n = 8$.

Let us consider DM production mechanisms. In order to suppress the baryonic isocurvature perturbation (see Eq. (33)), the reheating temperature is required as $T_{\text{RH}} \lesssim 1$ GeV for $n = 4$ flat direction with $\lambda \lesssim 10^{-10}$ or $n = 6, 8$ flat directions. In such a low reheating temperature, the two contributions, from the direct decay of the inflaton and from inelastic scatterings during the thermalization, explained in the previous subsection can generate DM, and the results is again given by Eqs. (55) and (67). In addition, the decay of Q-balls also generate a sizable DM abundance [16, 22–26, 32] because they decay after DM freezes out (see Eq. (82)).

In the rest of this subsection, we focus on a scenario of baryon and DM co-genesis from Q-ball decay. This scenario can be realized in the non-shaded region in Fig. 1 where the two contributions of DM abundance, from the direct decay of inflaton and from inelastic scatterings, are negligible. This is the case with, for example, a flat direction with $n = 8$ and $\lambda \lesssim 10^{-4}$.

As we have explained in Sec. IV, the decay rate of Q-ball is saturated and determined by the Pauli blocking effect. While SUSY particles are produced from the Q-ball surface only through elementary decay process like $\tilde{q} \rightarrow q + (\text{gaugino})$, quarks are dominantly produced through scattering process via gaugino or Higgsino exchange like $\tilde{q} + \tilde{q} \rightarrow q + q$ [53]. Thus, the ratio of the Q-ball decay into sparticles and quarks is calculated as

$$\frac{\text{Br}(\text{Q-ball} \rightarrow (\text{gauginos}))}{\text{Br}(\text{Q-ball} \rightarrow q)} \simeq \frac{n_s}{8n_q}, \quad (83)$$

where a factor of 8 is due to the difference of the elementary processes as we have explained in Sec. IV. The factor n_s is the effective number of sparticles into which Q-balls can decay. Since the flux of massive particles from a Q-ball surface is smaller than that of massless particles, there is a correction due to non-zero sparticle masses, which is derived in the Appendix. Thus we obtain

$$n_s = \sum_s g_s f(m_s/\omega_0), \quad (84)$$

where m_s is the mass of the sparticle s , g_s is the number of species for the sparticle and f is a function given in the Appendix. For example, $g_s = 1, 3$, and 8 for the bino, wino, and gluino, respectively.¹⁴ However, Q-balls can decay only into particles lighter than the energy

¹⁴ Note that g_s also depends on the flat direction. In the case of $\bar{u}d\bar{d}$ flat direction, Q-balls do not decay into winos, $g_{\text{wino}} = 0$, since they consists of only right-handed squarks [32].

of the Q-ball per unit charge, ω_0 , which is approximately equal to the mass of squarks at the energy scale of $|\phi|$ ($\sim 10^{15}$ GeV). In a typical model of gravity mediation, a mass of squarks at the energy scale of 10^{15} GeV is mostly smaller than the mass of the gluino and larger than that of the bino (LSP) [76]. Thus in the typical models Q-balls can decay into binos, and not into gluino.¹⁵ Depending on a model, Q-balls can also decay into winos and Higgsinos. Hereafter, we assume Q-balls can not decay into Higgsinos, for simplicity (see Ref. [76] for complete discussion).

Since all sparticles eventually decay into binos,¹⁶ we obtain the following formula for the baryon-to-DM ratio:

$$\frac{\Omega_{\text{DM}}}{\Omega_b} = \frac{m_{\tilde{b}}}{|b| m_p} \frac{n_s}{8n_q}, \quad (85)$$

$$\simeq \frac{m_{\tilde{b}}}{bm_p} \frac{\sum_s f(m_s/\omega_0)}{8n_q}. \quad (86)$$

We should emphasize that this ratio is independent of the reheating temperature and the charge of Q-balls. As an illustration, let us calculate two asymptotic solutions. When $m_s \ll \omega_0$, the function f approaches 1 (see the Appendix) and $n_s \simeq 12$, where we have included contributions from gauginos. On the other hand, if $m_{\tilde{b}} \rightarrow \omega_0$ with other particles mass larger than ω_0 , a combination of $m_{\tilde{b}}n_s/\omega_0$ approaches $4(1 - m_{\tilde{b}}/\omega_0)^3 \ll 1$. Thus we obtain two asymptotic solutions for the bino mass, which yields the correct ratio of DM and baryon density;

$$m_{\tilde{b}} \approx \begin{cases} 0.7n_q |b| m_p \frac{\Omega_{\text{DM}}}{\Omega_b} \simeq 10 \text{ GeV} & (\omega_0 \gg m_s) \\ \omega_0 \left[1 - \left(2n_q |b| \frac{\Omega_{\text{DM}} m_p}{\Omega_b \omega_0} \right)^{1/3} \right] & (m_{\tilde{b}} \rightarrow \omega_0), \end{cases} \quad (87)$$

where we assume $n_q = 10$ and $b = 1/3$ in the first line. The bino mass of 10 GeV is unrealistic for ordinary models in gravity mediation. We conclude that we can explain the observed baryon-to-DM ratio if the bino mass is close to below ω_0 .

In Fig. 2, we show the constraint on ω_0 and $m_{\tilde{b}}$. On the boundary of and inside the blue (dark gray) shaded region, the DM density produced by the decay of Q-balls is equal and larger than the observed value respectively. Here, we have assumed the grand unified theory (GUT) relation, where the masses of the wino and gluino are two and six times larger than that of the bino. Under the GUT relation, the red (light gray) shaded region is already

¹⁵ Even in this case Eq. (84) is valid since $f(x > 1) = 0$.

¹⁶ For the case of the axino LSP, see Refs. [25, 26].

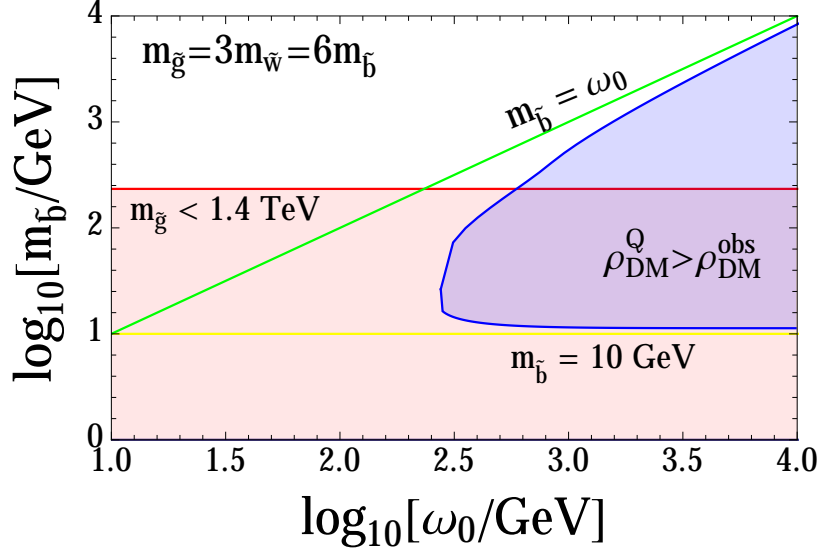


FIG. 2. Exclusion plot in a model of gravity mediation with Q-ball formation. We assume that the number of quarks interacting with Q-ball, n_q , is 10 and baryon charge of the AD field, b , is $-1/3$. We also assume that the masses of the wino and gluino are two and six times larger than that of the bino, which is a typical case in gravity mediation with the grand unified theory relation. The abundance of DM produced from Q-ball decay ($\rho_{\text{DM}}^{\text{Q}}$) is larger than that observed in the blue (dark gray) shaded region. In the red (light gray) shaded region, the gluino mass is smaller than 1.4 TeV and excluded by the gluino search at the ATLAS Collaboration [75]. The green-dotted and yellow-dashed lines indicate the limit of $m_{\tilde{b}} \rightarrow \omega_0$ and $m_{\tilde{b}} \rightarrow 10$ GeV, respectively.

excluded by the gluino search at the ATLAS Collaboration [75]. Detailed calculations in the constrained MSSM will be performed in the near future [76].

C. Gauge mediation without Q-ball

In models of gauge mediation, SUSY breaking in a hidden sector is transmitted to the standard model sector by gauge interactions mediated by a messenger sector. Since the AD field has some gauge charge, gauge fields acquire effective masses of the order of $g|\phi|$, where g generically stands for the Standard Model gauge coupling. The transmission of SUSY breaking effect is therefore suppressed for $g|\phi| \gg M_s$, where M_s is a messenger scale [77], and thereby the soft mass of the AD field is suppressed. The condition for Q-ball formation, Eq. (40), is therefore satisfied if there is no term in the potential of the AD field other than

the soft mass term. However, if the AD field is LH_u flat direction, the μ term of Higgs multiplets prevents the flat direction forming Q-balls [78].¹⁷ In this subsection, we consider the case of LH_u flat direction in gauge mediation and construct a consistent scenario to account for the observed DM density as well as baryon density.

Since the mass of the gravitino $m_{3/2}$ is much smaller than the electroweak scale, and since the AD field starts to oscillate at $H_{\text{osc}} \sim \mu \sim 1$ TeV, the ellipticity parameter defined in Eq. (23) is much smaller than one,

$$\epsilon \simeq 5 \times 10^{-3} \left(\frac{m_{3/2}}{5 \text{ GeV}} \right) \left(\frac{\mu}{1 \text{ TeV}} \right)^{-1}. \quad (88)$$

Taking into account $\Delta B_{\text{after sphaleron}} \simeq 0.3 \times \Delta(B - L)_{\text{before sphaleron}}$ due to the sphaleron effect [46] and $b = -1/2$ for $B - L$ charge of LH_u flat direction, we find that Eq. (33) is rewritten as

$$T_{\text{RH}} \simeq \begin{cases} 1 \times 10^8 \text{ GeV} \left(\frac{m_{3/2}}{6 \text{ GeV}} \right)^{-1} \left(\frac{\mu}{1 \text{ TeV}} \right) \left(\frac{\lambda}{10^{-4}} \right) & \text{for } n = 4, \\ 2 \times 10^5 \text{ GeV} \left(\frac{m_{3/2}}{8 \text{ MeV}} \right)^{-1} \left(\frac{\mu}{1 \text{ TeV}} \right)^{3/2} \left(\frac{\lambda}{10^{-4}} \right)^{1/2} & \text{for } n = 6, \\ 2 \times 10^4 \text{ GeV} \left(\frac{m_{3/2}}{0.9 \text{ MeV}} \right)^{-1} \left(\frac{\mu}{1 \text{ TeV}} \right)^{5/3} \left(\frac{\lambda}{10^{-4}} \right)^{1/3} & \text{for } n = 8. \end{cases} \quad (89)$$

Note that we assume a discrete R-symmetry which controls higher-dimensional terms in the superpotential as well as the term with $n = 2$. Therefore, in contrast to the case with the R-charge, LH_u flat direction with $n = 6$ or 8 is also possible.

Next, let us estimate the abundance of the gravitino, which is the LSP in gauge mediation. There are two contributions to the gravitino production, depending on the reheating temperature. If the reheating temperature is larger than the mass scale of MSSM particles, MSSM particles are in the thermal equilibrium and gravitinos are produced from thermal bath through scatterings between gluons and gluinos, as is discussed in Refs. [40, 79–82]. Here we quote the result from Ref. [79]:

$$\frac{\rho_{3/2}^{\text{th}}}{s} \simeq 0.4 \text{ eV} \left(\frac{T_{\text{RH}}}{10^8 \text{ GeV}} \right) \left(\frac{m_{\tilde{g}}}{1 \text{ TeV}} \right)^2 \left(\frac{m_{3/2}}{2 \text{ GeV}} \right)^{-1}. \quad (90)$$

where $m_{\tilde{g}}$ is the gluino mass. The parameter dependences of this result can be understood

¹⁷ In the model of seesaw mechanism, F term potential of right-handed neutrinos also lift LH_u flat direction.

Since an upper bound on isocurvature fluctuation requires large value of the AD field, the F term potential should be sufficiently small. The smallness is realized if right-handed neutrinos are light and/or one of left-handed neutrinos is light.

by

$$\frac{\rho_{3/2}^{\text{th}}}{s} \sim \frac{m_{3/2} \langle \sigma_{\text{scatt}} v \rangle n_r^2}{sH} \Big|_{T=T_{\text{RH}}}, \quad (91)$$

$$\langle \sigma_{\text{scatt}} v \rangle \sim \frac{g_3^2 m_{\tilde{g}}^2}{m_{3/2}^2 M_{\text{pl}}^2}, \quad (92)$$

where $n_r = \zeta(3)T^3/\pi^2$ is the number density of radiation in the thermal bath, and g_3 is a strong coupling constant.

If the reheating temperature is smaller than the mass scale of MSSM particles, MSSM particles are produced by the mechanism explained in Sec. V A. Then, MSSM particles eventually decay into gravitinos. The abundance of the gravitino is given by

$$\frac{\rho_{3/2}^{\text{inela}}}{s} = m_{3/2} \left(\frac{T_{\text{RH}}}{m_{\text{SUSY}}} \right)^3, \quad (93)$$

$$\simeq 0.3 \text{ eV} \left(\frac{T_{\text{RH}}}{5 \text{ GeV}} \right)^3 \left(\frac{m_{\text{SUSY}}}{5 \text{ TeV}} \right)^{-3} \left(\frac{m_{3/2}}{300 \text{ MeV}} \right), \quad (94)$$

where m_{SUSY} is the mass scale of MSSM particles whose production by inelastic process is efficient. Typically, m_{SUSY} can be identified with the mass of the NLSP. Note that if the NLSP is produced too much, its annihilation is effective and the gravitino abundance decreases accordingly. When the NLSP is right-handed stau, which is the case with typical gauge mediation models, its annihilation cross section is given as [83]

$$\langle \sigma_{\text{ann}} v \rangle_{\tilde{l}_R} \simeq 3 \times 10^{-11} \text{ GeV}^{-2} \left(\frac{m_{\tilde{l}_R}}{5 \text{ TeV}} \right)^{-2}, \quad (95)$$

where we have omitted bino mass dependence for simplicity. In analogy with the derivation of Eq. (68), the annihilation effect of the NLSP puts an upper bound on the gravitino abundance produced from the decay of the NLSP:

$$\begin{aligned} \frac{\rho_{\text{DM}}^{\text{inela (ann)}}}{s} &\simeq \sqrt{\frac{45}{8\pi^2 g_*}} \frac{m_{3/2}}{T_{\text{RH}} \langle \sigma_{\text{ann}} v \rangle M_{\text{pl}}}, \\ &\simeq 0.3 \text{ eV} \left(\frac{T_{\text{RH}}}{10 \text{ GeV}} \right)^{-1} \left(\frac{m_{3/2}}{1 \text{ GeV}} \right) \left(\frac{m_{\tilde{l}_R}}{5 \text{ TeV}} \right)^2. \end{aligned} \quad (96)$$

In summary, the gravitino abundance is given by

$$\frac{\rho_{3/2}}{s} \simeq \begin{cases} \frac{\rho_{3/2}^{\text{th}}}{s} & \text{for } T_{\text{RH}} \gtrsim m_{\text{SUSY}}, \\ \min \left[\frac{\rho_{\text{DM}}^{\text{inela}}}{s}, \frac{\rho_{\text{DM}}^{\text{inela (ann)}}}{s} \right] & \text{for } T_{\text{RH}} \ll m_{\text{SUSY}}. \end{cases} \quad (97)$$

Note that gravitinos and MSSM particles can be produced in inflaton decay as is discussed in Sec. V A. If the reheating temperature is lower than the mass scale of MSSM particles, the gravitino abundance is given by Eq. (55). We can neglect this contribution at least if $m_\phi \gtrsim 10^{12}$ GeV. On the other hand, if the reheating temperature is higher than the mass scale of MSSM particles, the MSSM particles are soon thermalized and Eq. (90) holds. The gravitino abundance produced in inflaton decay depends on the branching ratio of inflaton decay into gravitino. In this subsection, we assume that the branching into gravitino is so small that its abundance from inflaton decay is much less than the observed DM abundance.

In Fig. 3, we show the constraint on the gravitino mass and the reheating temperature. We assume that the mass of gluino is 2 TeV, $\mu = 1$ TeV, and $m_{\text{SUSY}} = m_{\text{NLSP}} = 1$ TeV. We also assume that the NLSP is right-handed stau and its annihilation cross section is given by Eq. (95). On the boundary of and inside the shaded region, the DM abundance is equal to and larger than that observed, respectively. In the red (light gray) shaded region, DM is produced from scatterings between gluons and gluinos. The upper bound on the blue (dark gray) shaded region is determined by the NLSP abundance produced through inelastic scatterings (that is, Eq. (94) with T_{RH} given by Eq. (89)), while the lower bound on that is determined by the annihilation of the NLSP (Eq. (96)). The (dashed) lines show the required reheating temperature and the gravitino mass for the successful Affleck-Dine Baryogenesis, for $n = 4, 6,$ and 8 with $\lambda = 10^{-4}$ (10^{-6}).

If the DM abundance is produced by scatterings from thermal bath (the lower boundary of the red (light gray) shaded region in Fig. 3), from Eqs. (89) and (90), the mass of the gravitino is predicted to be

$$m_{3/2} \simeq \left(\frac{\mu}{1 \text{ TeV}} \right) \left(\frac{m_{\tilde{g}}}{2 \text{ TeV}} \right) \times \begin{cases} 8 \text{ GeV} \left(\frac{\lambda}{10^{-4}} \right)^{1/2} & \text{for } n = 4. \\ 10 \text{ MeV} \left(\frac{\lambda}{10^{-4}} \right)^{1/4} & \text{for } n = 6, \\ 1 \text{ MeV} \left(\frac{\lambda}{10^{-4}} \right)^{1/7} & \text{for } n = 8. \end{cases} \quad (98)$$

The case with $n = 4$ and $\lambda \sim 10^{-4}$ requires large gravitino mass. The large gravitino mass contributes to electric dipole moments (EDMs) through supergravity effect in general. For gravitino mass larger than $\mathcal{O}(100)$ MeV, suppression of CP phases due to the supergravity effect is necessary [84].

Let us consider the case where the DM abundance is explained by the contribution from inelastic scatterings during the thermalization process (the boundary of the blue (dark gray)

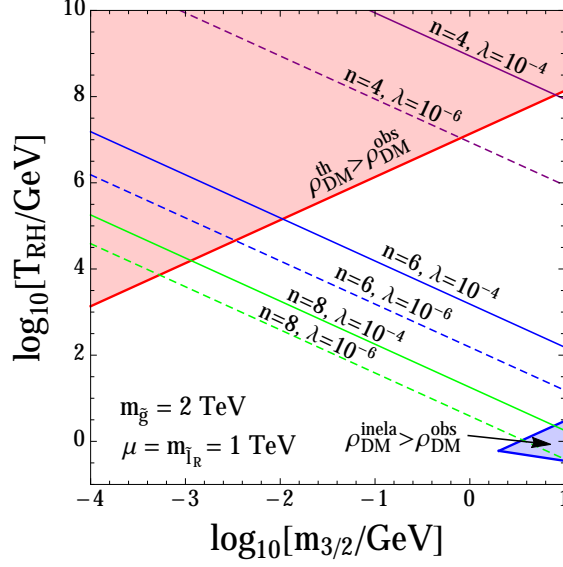


FIG. 3. Exclusion plot in a model of gauge mediation without Q-ball formation. We assume that the mass of gluino is 2 TeV, $\mu = 1$ TeV, and $m_{\text{SUSY}} = m_{\text{NLSP}} = 1$ TeV. We also assume that the NLSP is right-handed stau and its annihilation cross section is given by Eq. (95). The abundance of DM produced from scatterings between gluon and gluinos in the thermal bath ($\rho_{\text{DM}}^{\text{th}}$) is larger than that observed in the red (light gray) shaded region. In the blue (dark gray) shaded region, the abundance of DM produced by the decay of the NLSP produced through inelastic scatterings during the thermalization process exceeds the observed one. The (dashed) lines are the reheating temperature required by the success of the Affleck-Dine baryogenesis for $n = 4, 6$, and $n = 8$ flat direction with $\lambda = 10^{-4}$ (10^{-6}).

shaded region in Fig. 3), focusing on the free-streaming velocity of the gravitino. The NLSP decays into gravitinos with a decay rate given by

$$\Gamma_{\text{NLSP}} \simeq \frac{m_{\text{NLSP}}^5}{48\pi m_{3/2}^2 M_{\text{pl}}^2}. \quad (99)$$

The decay temperature of the NLSP is thus given by

$$T_{\text{NLSP}} \simeq 0.3 \text{ GeV} \left(\frac{m_{\text{NLSP}}}{5 \text{ TeV}} \right)^{5/2} \left(\frac{m_{3/2}}{0.2 \text{ GeV}} \right)^{-1}. \quad (100)$$

The present-day free-streaming velocity of the gravitino DM is calculated as [27, 85, 86]

$$v_0 \simeq \frac{m_{\text{NLSP}}/2}{m_{3/2}} \frac{T_0}{T_{\text{NLSP}}} \left(\frac{g_{*s}(T_0)}{g_{*s}(T_{\text{NLSP}})} \right)^{1/3}, \quad (101)$$

$$\simeq 9 \times 10^{-9} \left(\frac{m_{\text{NLSP}}}{5 \text{ TeV}} \right)^{-3/2} \left(\frac{g_{*s}(T_0)}{g_{*s}(T_{\text{NLSP}})} \right)^{1/3}, \quad (102)$$

where T_0 ($\simeq 2.3 \times 10^{-4}$ eV) is the temperature at the present time, and g_{*s} is the effective number of relativistic degrees of freedom for entropy. The observation of the Lyman- α forest puts an upper bound on the free-streaming velocity as $v_0 \lesssim 2.5 \times 10^{-8}$ [87] (see Ref. [86] for review). This results in $m_{\text{NLSP}} \gtrsim 3$ TeV from Eq. (102). It is expected that future observations of redshifted 21 cm line would improve the upper bound to $v_0 \lesssim 2 \times 10^{-9}$ [88]. Hence this scenario would be tested by future observations of redshifted 21 cm line if the mass of the NLSP is less than about 14 TeV.

Finally, we comment on the BBN bound on the gravitino mass [89, 90]. Since the NLSP is long-lived in gauge mediation, they may produce high energy hadrons or photons after the BBN epoch. These high energy particles induce hadro- and photo-dissociation processes of light elements, which spoil the success of the BBN scenario. This puts a stringent lower bound on the NLSP mass especially for the case of $m_{3/2} \gtrsim 1$ GeV. When the NLSP is the stau, which is a typical case in gauge mediation, the NLSP mass has to be larger than about 700 GeV for $m_{3/2} \simeq 10$ GeV [90].

D. Gauge mediation with Q-balls

In this subsection, we consider a flat direction other than LH_u flat direction. As explained in the previous subsection, the soft mass term for the AD field is absent for a VEV larger than the messenger scale because the transmission of SUSY breaking effect is suppressed for such a large VEV. Thus we obtain the following potential for the AD field [77]:

$$V = \begin{cases} m_\phi^2 |\phi|^2 & \text{for } g|\phi| \ll M_s, \\ M_F^4 \left[\log \frac{g^2 |\phi|^2}{M_s^2} \right]^2 & \text{for } g|\phi| \gg M_s, \end{cases} \quad (103)$$

where M_s is a messenger mass, and g generically stands for the Standard-Model gauge coupling. A parameter M_F^2 is proportional to the VEV of the F component of a gauge-singlet chiral multiplet in the messenger sector as

$$M_F^2 = \frac{m_\phi^2 M_s^2}{g^2} = \frac{gy}{(4\pi)^2} \langle F_s \rangle, \quad (104)$$

where y is a coupling constant for the interaction between the gauge singlet chiral multiplet and the messenger field. The mass of the gravitino is related to the SUSY breaking F -term

as

$$\langle F_s \rangle = k\sqrt{3}m_{3/2}M_{\text{pl}}, \quad (105)$$

$$k \leq 1, \quad (106)$$

where a factor k is less than one when the messenger sector indirectly couple to the SUSY breaking sector. Hereafter we redefine the combination of yk as k ($\lesssim 1$).

Since the curvature of the potential at the energy scale of $|\phi_{\text{osc}}|$ is roughly given by $M_F^2/|\phi_{\text{osc}}|$, the AD field begins to oscillate at the time of $H_{\text{osc}} \sim M_F^2/|\phi_{\text{osc}}|$ ($\sim \omega_0$). Using this and Eqs. (32), (104), and (105), the VEV of the AD field at the beginning of its oscillation is calculated as

$$|\phi_{\text{osc}}| \simeq \begin{cases} 3 \times 10^{13} k^{1/3} \left(\frac{m_{3/2}}{1 \text{ GeV}}\right)^{1/3} \left(\frac{\lambda}{10^{-6}}\right)^{-1/3}, & \text{for } n = 4, \\ 10^{15} k^{1/5} \left(\frac{m_{3/2}}{1 \text{ GeV}}\right)^{1/5} \left(\frac{\lambda}{10^{-4}}\right)^{-1/5}, & \text{for } n = 6, \\ 10^{16} k^{1/7} \left(\frac{m_{3/2}}{1 \text{ GeV}}\right)^{1/7} \left(\frac{\lambda}{10^{-4}}\right)^{-1/7}, & \text{for } n = 8. \end{cases} \quad (107)$$

We can calculate the ellipticity parameter ϵ ($\simeq m_{3/2}/H_{\text{osc}}$) and the required reheating temperature as

$$\epsilon \simeq \begin{cases} 10^{-3} k^{-2/3} \left(\frac{m_{3/2}}{1 \text{ GeV}}\right)^{1/3} \left(\frac{\lambda}{10^{-6}}\right)^{-1/3}, & \text{for } n = 4, \\ 4 \times 10^{-2} k^{-4/5} \left(\frac{m_{3/2}}{1 \text{ GeV}}\right)^{1/5} \left(\frac{\lambda}{10^{-4}}\right)^{-1/5}, & \text{for } n = 6, \\ 0.4 k^{-6/7} \left(\frac{m_{3/2}}{1 \text{ GeV}}\right)^{1/7} \left(\frac{\lambda}{10^{-4}}\right)^{-1/7}, & \text{for } n = 8, \end{cases} \quad (108)$$

and

$$T_{\text{RH}} \simeq \begin{cases} 3 \times 10^6 \text{ GeV } k^{2/3} \left(\frac{m_{3/2}}{1 \text{ GeV}}\right)^{-1/3} \left(\frac{\lambda}{10^{-6}}\right)^{4/3}, & \text{for } n = 4, \\ 3 \text{ GeV } k^{6/5} \left(\frac{m_{3/2}}{1 \text{ GeV}}\right)^{1/5} \left(\frac{\lambda}{10^{-4}}\right)^{4/5}, & \text{for } n = 6, \\ 0.5 \text{ MeV } k^{10/7} \left(\frac{m_{3/2}}{1 \text{ GeV}}\right)^{3/7} \left(\frac{\lambda}{10^{-4}}\right)^{4/7}, & \text{for } n = 8, \end{cases} \quad (109)$$

respectively. For $n = 8$ flat direction, the reheating temperature is so small that the success of the BBN is spoiled. Hereafter, we consider only the cases with $n = 4$ and 6.

The reheating temperature for $n = 4$ flat direction may be so large that gravitino is produced from the thermal plasma. From Eq. (90), we obtain the gravitino abundance produced from the thermal plasma as

$$\frac{\rho_{3/2}^{\text{th}}}{s} \simeq 0.1 \text{ eV } k^{2/3} \left(\frac{m_{\tilde{g}}}{2 \text{ TeV}}\right)^2 \left(\frac{m_{3/2}}{1 \text{ GeV}}\right)^{-4/3} \left(\frac{\lambda}{10^{-6}}\right)^{4/3} \quad \text{for } n = 4. \quad (110)$$

Although gravitinos and MSSM particles can be produced from inflaton decay directly in the same way in Sec. V A, we neglect its contribution assuming a large inflaton mass. For

$n = 6$ flat direction, the reheating temperature is smaller than the freeze-out temperature of the NLSP and thus the NSLPs are produced at the reheating epoch as explained in the previous subsection (see Eq. (94)). This is also the case with $n = 4$ and $\lambda \ll 10^{-9}$. Since the NLSPs may annihilate and eventually decay into gravitinos, the abundance of the gravitino is again given by the second line of Eq. (97) with the reheating temperature of Eq. (109).

Thus we obtain the abundance of the gravitino as

$$\frac{\rho_{3/2}^{\text{inela}}}{s} \simeq \begin{cases} 4 \text{ eV } k^2 \left(\frac{m_{\text{NLSP}}}{10 \text{ TeV}}\right)^{-3} \left(\frac{\lambda}{10^{-10}}\right)^4 & \text{for } n = 4, \\ 0.2 \text{ eV } k^{18/5} \left(\frac{m_{\text{NLSP}}}{5 \text{ TeV}}\right)^{-3} \left(\frac{m_{3/2}}{1 \text{ GeV}}\right)^{8/5} \left(\frac{\lambda}{10^{-4}}\right)^{12/5} & \text{for } n = 6, \end{cases} \quad (111)$$

with an upper bound due to the annihilation of the NLSP as

$$\frac{\rho_{3/2}^{\text{inela (ann)}}}{s} \simeq \begin{cases} 0.4 \text{ eV } k^{-2/3} \left(\frac{m_{3/2}}{1 \text{ GeV}}\right)^{4/3} \left(\frac{m_{\text{NLSP}}}{7 \text{ TeV}}\right)^2 \left(\frac{\lambda}{10^{-10}}\right)^{-4/3} & \text{for } n = 4, \\ 0.4 \text{ eV } k^{-6/5} \left(\frac{m_{3/2}}{1 \text{ GeV}}\right)^{4/5} \left(\frac{m_{\text{NLSP}}}{3 \text{ TeV}}\right)^2 \left(\frac{\lambda}{10^{-4}}\right)^{-4/5} & \text{for } n = 6. \end{cases} \quad (112)$$

In addition, Q-balls may provide another source of gravitinos as shown below.

For the potential in Eq. (103), there exists a Q-ball solution, approximated to be [91]^{18,19}

$$\phi(r, t) \simeq \begin{cases} \frac{1}{\sqrt{2}} \phi_0 \frac{\sin(\omega_0 r)}{\omega_0 r} e^{-i\omega_0 t} & \text{for } r \leq R \equiv \frac{\pi}{\omega_0}, \\ 0 & \text{for } r > R, \end{cases} \quad (113)$$

where ω_0 and ϕ_0 are given as

$$\omega_0 \simeq \sqrt{2\pi} M_F Q^{-1/4}, \quad (114)$$

$$\phi_0 \simeq M_F Q^{1/4}. \quad (115)$$

We omit $\mathcal{O}(1)$ logarithmic corrections on Q-ball parameters for simplicity [94]. Since the energy of the Q-ball is calculated as

$$M_Q \simeq \frac{4\sqrt{2}\pi}{3} M_F Q^{3/4}, \quad (116)$$

the energy of the Q-ball per unit charge dM_Q/dQ is approximated to be ω_0 .

¹⁸ If ϕ_{osc} or ϕ_0 is less than about the messenger mass M_s ($\simeq gM_F^2/m_\phi$), the suppression on the transmission of SUSY breaking effect is absent and the situation is similar to models of gravity mediation [28, 92]. We have checked that ϕ_{osc} and ϕ_0 is larger than M_s in the case we are interested in, if the mass of the AD field m_ϕ is larger than 10 TeV or that of gravitino $m_{3/2}$ is less than 10 GeV.

¹⁹ If $\phi_0 \gtrsim M_F^2/m_{3/2}$, the potential of the AD field is dominated by the soft mass of the form $m_{3/2}^2|\phi|^2$, which is induced by gravity mediated SUSY breaking effect. In this case, a Q-ball solution is known as a ‘‘new type Q-ball’’ [93], which is stable and is a DM candidate for the case of $m_{3/2}/|b| \lesssim 1 \text{ GeV}$. In this paper, we focus on the case of the LSP DM and leave that case for a future work. Note that if $k \sim 1$, a ‘‘new type Q-ball’’ is never formed.

Using $R \simeq \pi/\omega_0$ and $\omega_0 \sim M_F^2/\phi$ in Eq. (41), a typical charge of Q-balls formed after the Affleck-Dine baryogenesis is estimated as

$$Q \sim \beta \left(\frac{|\phi_{\text{osc}}|}{M_F} \right)^4, \quad (117)$$

$$\simeq \begin{cases} 10^{21} k^{-2/3} \left(\frac{m_{3/2}}{1 \text{ GeV}} \right)^{-2/3} \left(\frac{\lambda}{10^{-9}} \right)^{-4/3} & \text{for } n = 4, \\ 8 \times 10^{21} k^{-6/5} \left(\frac{m_{3/2}}{10 \text{ GeV}} \right)^{-6/5} \left(\frac{\lambda}{10^{-4}} \right)^{-4/5} & \text{for } n = 6, \end{cases} \quad (118)$$

where β has been calculated as 6×10^{-5} for $\epsilon \ll 1$ by the numerical simulation of Q-ball formation [19]. We have used Eq. (107) in the last line.²⁰ From Eqs. (45) and (118), the Q-ball decay temperature is calculated as

$$T_{\text{decay}} \simeq \begin{cases} 7 \text{ GeV } k^{2/3} \left(\frac{m_{3/2}}{1 \text{ GeV}} \right)^{2/3} \left(\frac{\lambda}{10^{-9}} \right)^{5/6}, & \text{for } n = 4, \\ 3 \text{ GeV } k \left(\frac{m_{3/2}}{10 \text{ GeV}} \right) \left(\frac{\lambda}{10^{-4}} \right)^{1/2}, & \text{for } n = 6, \end{cases} \quad (119)$$

where we use $\tilde{R} \simeq R = \pi/\omega_0$ and also use Eqs. (104), (105), and (114) to eliminate ω_0 and M_F . We thus find that Q-balls decay after the NLSP freezes out for $n = 4$ with $\lambda \lesssim 10^{-8}$ and $n = 6$.

Now, let us calculate the NLSP abundance from Q-ball decay, which is another source of gravitinos. A detailed analysis has been done in Ref. [31] (see also Ref. [29, 30]), where gravitino production from the direct decay of Q-balls via Planck-suppressed operators [27–29, 31] is taken into account. There, the ellipticity parameter ϵ is regarded as a free parameter. In this paper, we use $\epsilon = m_{3/2}/H_{\text{osc}}$ without fine-tuning. In this case, gravitinos directly produced in Q-ball decay is too inefficient to account for the observed DM density.

Q-balls decay into quarks at $T = T_{\text{decay}}$ and lose their charges. Since the energy of Q-ball per unit charge, ω_0 , is proportional to $Q^{-1/4}$ (see Eq. (114)), a Q-ball can decay into the next-to-lightest SUSY particle (NLSP) once its charge decreases down to $Q_{\text{cr}} \equiv (\sqrt{2}\pi M_F/m_{\text{NLSP}})^4$, where m_{NLSP} is the mass of the NLSP.²¹ Thus we estimate the total number of the NLSP from the decay of each Q-ball as

$$n_{\text{NLSP}} = \begin{cases} B_{\text{NLSP}} & \text{for } \omega_0 > m_{\text{NLSP}}, \\ B_{\text{NLSP}} \frac{Q_{\text{cr}}}{Q} & \text{for } \omega_0 < m_{\text{NLSP}}, \end{cases} \quad (120)$$

²⁰ Q-balls with baryon charge less than about 10^{18} is completely disappeared by the dissipation effect in the thermal plasma [95, 96] (see also Ref. [19]). In this case Q-balls do not affect the DM abundance.

²¹ In the case of $\bar{u}d\bar{d}$ flat direction, Q-balls does not interact with sleptons and thus cannot decay into them.

In this case, the mass of the NLSP for the condition $\omega_0 \lesssim m_{\text{NLSP}}$ in Eq. (120) has to be replaced with that of the lightest MSSM particle which Q-balls can decay into.

where the branching into the NLSP, Br_{NLSP} , is of the order of 0.01. The first line is for the case that Q-balls can decay into the NLSP from the beginning, while the second one is for the case that Q-balls can decay into the NLSP only after their charges decrease down to Q_{cr} . The combination of Q_{cr}/Q is rewritten as

$$\frac{Q_{\text{cr}}}{Q} \equiv \frac{1}{Q} \left(\frac{\sqrt{2}\pi M_F}{m_{\text{NLSP}}} \right)^4, \quad (121)$$

$$\simeq \begin{cases} 3 k^{8/3} \left(\frac{m_{3/2}}{2 \text{ GeV}} \right)^{8/3} \left(\frac{\lambda}{10^{-9}} \right)^{4/3} \left(\frac{m_{\text{NLSP}}}{5 \text{ TeV}} \right)^{-4}, & \text{for } n = 4, \\ 5 k^{16/5} \left(\frac{m_{3/2}}{10 \text{ GeV}} \right)^{16/5} \left(\frac{\lambda}{10^{-4}} \right)^{4/5} \left(\frac{m_{\text{NLSP}}}{5 \text{ TeV}} \right)^{-4}, & \text{for } n = 6. \end{cases} \quad (122)$$

We find that $Q_{\text{cr}}/Q > 1$ for relatively large gravitino mass. The number density of the NLSP from Q-ball decay is then given as

$$\frac{n_{\text{NLSP}}^{\text{decay}}}{s} \simeq \text{fr}_N \frac{n_\phi}{s} \simeq \text{fr}_N \frac{Y_b}{\epsilon b}. \quad (123)$$

If these NLSPs do not annihilate, the gravitino abundance from the Q-ball through the NLSP decay is given as

$$\frac{\rho_{3/2}^{\text{decay}}}{s} \simeq m_{3/2} \text{fr}_N \frac{Y_b}{\epsilon b}, \quad (124)$$

$$\simeq \begin{cases} 0.4 \text{ eV } k^{2/3} \left(\frac{\text{fr}_N}{0.01} \right) \left(\frac{m_{3/2}}{2 \text{ GeV}} \right)^{2/3} \left(\frac{\lambda}{10^{-9}} \right)^{1/3}, & \text{for } n = 4, \\ 0.5 \text{ eV } k^{4/5} \left(\frac{\text{fr}_N}{0.01} \right) \left(\frac{m_{3/2}}{10 \text{ GeV}} \right)^{4/5} \left(\frac{\lambda}{10^{-4}} \right)^{1/5}, & \text{for } n = 6. \end{cases} \quad (125)$$

The NLSPs produced from Q-balls are soon thermalized and may annihilate. We assume that the NLSP is right-handed stau and hence its annihilation cross section is given by Eq. (95). The annihilation effect of the NLSP results in the upper bound on the NLSP abundance given by

$$\frac{n_{\text{NLSP}}^{\text{decay (ann)}}}{s} \simeq \sqrt{\frac{45}{8\pi^2 g_*}} \frac{1}{T_{\text{decay}} \langle \sigma_{\text{ann}} v \rangle_{\tilde{l}_R} M_{\text{pl}}}, \quad (126)$$

$$\simeq \begin{cases} 0.6 \text{ eV } k^{-2/3} m_{3/2}^{-1} \left(\frac{m_{3/2}}{2 \text{ GeV}} \right)^{1/3} \left(\frac{\lambda}{10^{-9}} \right)^{-5/6} \left(\frac{m_{\text{NLSP}}}{5 \text{ TeV}} \right)^2, & \text{for } n = 4, \\ 0.4 \text{ eV } k^{-1} m_{3/2}^{-1} \left(\frac{\lambda}{10^{-4}} \right)^{-1/2} \left(\frac{m_{\text{NLSP}}}{1 \text{ TeV}} \right)^2, & \text{for } n = 6. \end{cases} \quad (127)$$

The gravitino abundance from the Q-ball through the NLSP decay is given by $\rho_{3/2}^{\text{decay (ann)}} = m_{3/2} n_{\text{NLSP}}^{\text{decay (ann)}}$.

To sum up, the gravitino abundance is given by

$$\frac{\rho_{3/2}}{s} \simeq \frac{\rho_{3/2}^{\text{th}}}{s} + \min \left[\frac{\rho_{3/2}^{\text{inela}}}{s}, \frac{\rho_{3/2}^{\text{inela (ann)}}}{s} \right] + \min \left[\frac{\rho_{3/2}^{\text{decay}}}{s}, \frac{\rho_{3/2}^{\text{decay (ann)}}}{s} \right], \quad (128)$$

where $\rho_{3/2}^{\text{th}}$ is absent for the case of $n = 6$. We show the results in Figs. 4 and 5. Inside blue (dark gray) shaded region, the gravitino abundance produced through inelastic scatterings during the reheating epoch is larger than the observed DM abundance. In the green (middle gray) shaded region, the abundance of DM produced from Q-ball decay mediated by the NLSP ($\rho_{3/2}^{\text{decay}}$) is larger than that observed. Q-balls can decay into the NLSPs from the first time (that is, $\omega_0 > m_{\text{NLSP}}$) below the green line. The lower boundary of the blue (dark gray) and green (middle gray) shaded regions are determined by the annihilation of the NLSP (Eqs. (112) and (127)). In the red (light gray) shaded region, the abundance of DM produced from the thermal plasma ($\rho_{3/2}^{\text{th}}$) is larger than that observed. The DM abundance is consistent with that observed on the boundary of the non-shaded regions.

We find that the gravitino mass has to be larger than $\mathcal{O}(1)$ GeV to account for the observed baryon and DM abundance for the case of $n = 6$. For the case of $n = 4$, while the DM abundance can be explained by the gravitino production from the thermal plasma in any value of gravitino mass, the gravitino production from Q-ball decay mediated by the NLSP can account for the DM abundance only if $m_{3/2} \gtrsim \mathcal{O}(1)$ GeV. As we have mentioned, this large value of the gravitino mass in general induces EDMs [84], which will be detected in near future unless CP phases due to supergravity effect is suppressed by some reasons or tunings. In addition, since gravitinos are produced from the NLSP decay, the gravitino DM obtains a sizable free-streaming velocity derived by Eq. (102). This again constraints the mass of the NLSP as $m_{\text{NLSP}} \gtrsim 3$ TeV [87], and also this scenario would be tested by future observations of redshifted 21 cm line if $m_{\text{NLSP}} \lesssim 14$ TeV [88].

VI. SUMMARY AND CONCLUSIONS

We have proposed scenarios which account for the observed baryon asymmetry and DM density in models of gravity and gauge mediation, taking into account an implication on the energy scale of inflation $H_{\text{inf}} \simeq 10^{14}$ GeV by the recent result of the BICEP2 experiment [1]. We have considered the Affleck-Dine baryogenesis without Hubble induced A -term potentials, which is indeed the case for most models of high-scale inflation in supergravity [9, 44, 45] and for D -term inflation [6–8]. In this case, the Affleck-Dine baryogenesis is excluded by an experimental upper bound on baryonic isocurvature perturbation, unless the initial phase of the AD field is tuned or the VEV of the AD field is as large as the Planck scale during

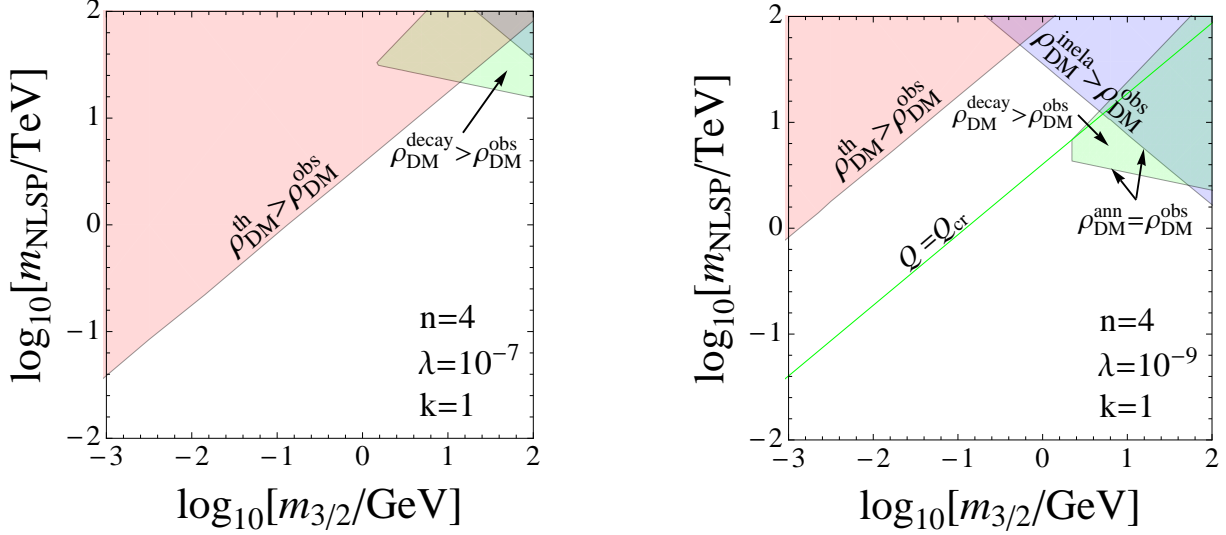


FIG. 4. Exclusion plot in a model of gauge mediation with Q-ball formation. We assume that $n = 4$ and $k = 1$. We also assume that $\lambda = 10^{-7}$ (left panel) and 10^{-9} (right panel). In the green (middle gray) shaded region, the abundance of DM produced from Q-ball decay mediated by the NLSP ($\rho_{3/2}^{\text{decay}}$) is larger than that observed. In the blue (dark gray) shaded region, the NLSP is produced too much through inelastic scatterings during the reheating epoch, that is, $\rho_{3/2}^{\text{inela}} > \rho_{\text{DM}}^{\text{obs}}$. In the red (light gray) shaded region, the abundance of DM produced from the thermal plasma ($\rho_{3/2}^{\text{th}}$) is larger than that observed. Here we have assumed that the mass of the gluino is five times larger than that of the NLSP. The lower boundaries of blue (dark gray) and green (middle gray) shaded regions are determined by the annihilation effect of the NLSP. The DM abundance is consistent with that observed at the boundary of the non-shaded regions. Q-balls can decay into the NLSPs from the first time (that is, $Q < Q_{\text{cr}}$) below the green line.

inflation. We have investigated the latter possibility in detail.

Since the AD field with large VEV results in larger energy density ratio for AD field/inflaton, it indicates lower reheating temperature of the Universe to account for the present baryon density successfully without additional entropy production. Hence, this scenario predicts a relatively low reheating temperature. When the reheating temperature is low, DM is dominantly produced in non-thermal processes. Therefore, it is necessary to investigate the non-thermal processes in detail. In addition, the Affleck-Dine baryogenesis often results in formation of Q-balls, which decay into light SUSY particles as well as quarks at later time. Based on these issues, we have constructed consistent scenarios to account

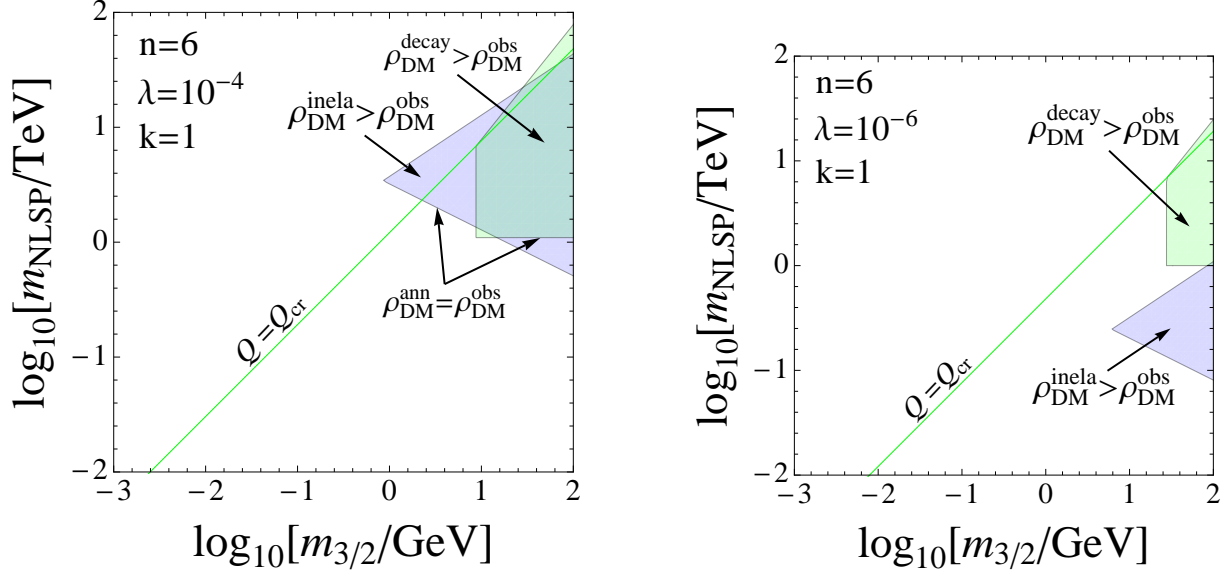


FIG. 5. Same as Fig. 4 but with $n = 6$. We assume that $\lambda = 10^{-4}$ (left panel) and 10^{-6} (right panel).

for the observed baryon and DM densities in the cases with and without Q-ball formation in models of gravity and gauge mediation.

In gravity mediation, DM is produced mainly from two sources: direct decay of inflaton into MSSM particles [34–39] and inelastic scatterings during reheating process [33, 34]. While the former process depends on unknown inflaton mass, the latter process depends only on the reheating temperature and DM mass. From the observation of the DM abundance, we have predicted the DM mass around the TeV scale. In addition, if Q-balls are formed after the Affleck-Dine baryogenesis, they emit gauginos lighter than squarks and thus they can be another source of DM. Interestingly, since the Pauli blocking effect at the Q-ball surface gives a simple relation between the branching into quarks and gauginos from Q-ball decay, we can overcome the baryon-DM coincidence problem in this scenario [32]. We have predicted the mass of the bino, which is the LSP in typical gravity mediation models, as $\mathcal{O}(1)$ TeV. These scenarios would be tested by direct detection experiments in the near future [34].

In gauge mediation, gravitino DM is produced by scatterings between gluon and gluino in the thermal bath at the reheating epoch [40]. We have confirmed that the baryon and DM density can be simultaneously explained in the Affleck-Dine baryogenesis when the mass of the gravitino is about $\mathcal{O}(1)$ MeV or $\mathcal{O}(1)$ GeV, depending on the power of superpotential for the AD field. However, any flat directions other than LH_u fragment into Q-balls after the

Affleck-Dine baryogenesis. Then Q-balls decay into NLSPs as well as quarks and the NLSPs eventually decay into gravitinos [30, 31]. We have found that this scenario can also explain the observed DM density, and have predicted that the gravitino and the NLSP masses are larger than about $\mathcal{O}(1)$ GeV and 3 TeV, respectively. The lower bound on the NLSP mass comes from an upper bound on the present-day free-streaming velocity of DM. This scenario would be tested by future observations of redshifted 21 cm line if the NLSP mass is less than about 14 TeV. The gravitino mass of $\mathcal{O}(1)$ GeV induces detectable EDMs in near future experiments unless CP phases due to supergravity effect is suppressed by some reasons or tunings.

ACKNOWLEDGEMENTS

K.H. thanks Norimi Yokozaki for useful discussion. This work is supported by a Grant-in-Aid for Scientific Research from the Ministry of Education, Science, Sports, and Culture (MEXT), Japan, No. 25400248 (M.K.) and No. 21111006 (M.K.), the World Premier International Research Center Initiative (WPI Initiative), MEXT, Japan (A.K., M.K. and M.Y.), the Program for Leading Graduate Schools, MEXT, Japan (M.Y.), and JSPS Research Fellowships for Young Scientists (K.H., K.M. and M.Y.).

Appendix: Q-ball decay rate into massive particles

In this appendix, we discuss the Q-ball decay rate into a massive particle χ [32]. While flux of a massless particle at the Q-ball surface is calculated as in Eq. (43), that of a massive particle is suppressed by its mass. Here we consider the Q-ball decay through an elementary process $\tilde{q} \rightarrow q + \chi$. We denote the mass of χ as m_χ . Since the total energy of this process is given by the energy of the Q-ball per unit charge, ω_0 , the particle χ obtains energy in the range of $[m_\chi, \omega_0]$ and the quark obtains energy in the range of $[0, \omega_0 - m_\chi]$. Their flux is determined by the following procedure. Due to conservation of energy and angular momentum, quark flux with the energy of E have to coincide with χ flux with the energy of $\omega_0 - E$. Since either of them cannot exceed upper bound on their flux due to the Pauli blocking effect, their flux is determined by the severer bound. The quark flux with the energy of E is proportional to $dp_{\text{quark}} = dE$, while the χ flux with the energy of $\omega_0 - E$ is

proportional to $v_\chi \times dp_\chi = p_\chi/E \times E/p_\chi dE = dE$, where we use $p_\chi^2 = (\omega_0 - E)^2 - m_\chi^2$. We obtain their flux at the Q-ball surface as

$$\mathbf{n} \cdot \mathbf{j}_\chi \simeq \frac{1}{8\pi^2} \int_0^{\omega_0 - m_\chi} dE \min [E^2, (\omega_0 - E)^2 - m_\chi^2]. \quad (\text{A.1})$$

This integral can be performed analytically and we obtain the following correction to the flux given in Eq. (43):

$$\mathbf{n} \cdot \mathbf{j}_\chi \simeq \frac{\omega_0^3}{96\pi^2} \times f(m_\chi/\omega_0), \quad (\text{A.2})$$

$$f(x) \equiv \begin{cases} 1 - 6x^2 + 8x^3 - 3x^4 & \text{for } 0 \leq x \leq 1 \\ 0 & \text{for } 1 < x \end{cases} \quad (\text{A.3})$$

Note that while the flux of sparticles is given by the above formula, the flux of quarks takes a different form $8 \times \omega_0^3/(96\pi^2)$, because they are produced through scattering process inside the Q-ball (see the discussion below Eq. (43)).

-
- [1] P. A. R. Ade *et al.* [BICEP2 Collaboration], arXiv:1403.3985 [astro-ph.CO].
 - [2] M. Bastero-Gil, A. Berera, R. O. Ramos and J. G. Rosa, Phys. Lett. B **712**, 425 (2012) [arXiv:1110.3971 [hep-ph]].
 - [3] M. Bastero-Gil, A. Berera, R. O. Ramos and J. G. Rosa, arXiv:1404.4976 [astro-ph.CO].
 - [4] I. Affleck and M. Dine, Nucl. Phys. B **249**, 361 (1985).
 - [5] M. Dine, L. Randall and S. D. Thomas, Nucl. Phys. B **458**, 291 (1996). [hep-ph/9507453].
 - [6] K. Enqvist and J. McDonald, Phys. Rev. Lett. **83**, 2510 (1999) [hep-ph/9811412].
 - [7] K. Enqvist and J. McDonald, Phys. Rev. D **62**, 043502 (2000) [hep-ph/9912478].
 - [8] M. Kawasaki and F. Takahashi, Phys. Lett. B **516**, 388 (2001) [hep-ph/0105134].
 - [9] S. Kasuya, M. Kawasaki and F. Takahashi, JCAP **0810**, 017 (2008) [arXiv:0805.4245 [hep-ph]].
 - [10] T. Higaki, K. S. Jeong and F. Takahashi, arXiv:1403.4186 [hep-ph].
 - [11] D. J. E. Marsh, D. Grin, R. Hlozek and P. G. Ferreira, arXiv:1403.4216 [astro-ph.CO].
 - [12] L. Visinelli and P. Gondolo, arXiv:1403.4594 [hep-ph].
 - [13] A. G. Dias, A. C. B. Machado, C. C. Nishi, A. Ringwald and P. Vaudrevange, arXiv:1403.5760 [hep-ph].
 - [14] A. Kusenko, Phys. Lett. **B405** (1997) 108.

- [15] A. Kusenko and M. E. Shaposhnikov, Phys. Lett. B **418**, 46 (1998).
- [16] K. Enqvist and J. McDonald, Phys. Lett. B **425**, 309 (1998); Nucl. Phys. B **538**, 321 (1999).
- [17] S. Kasuya and M. Kawasaki, Phys. Rev. D **61**, 041301(R) (2000).
- [18] S. Kasuya and M. Kawasaki, Phys. Rev. D **62**, 023512 (2000).
- [19] S. Kasuya and M. Kawasaki, Phys. Rev. D **64**, 123515 (2001).
- [20] S. Coleman, Nucl. Phys. **B262** (1985) 263.
- [21] A. G. Cohen, S. R. Coleman, H. Georgi and A. Manohar, Nucl. Phys. B **272**, 301 (1986).
- [22] M. Fujii and K. Hamaguchi, Phys. Lett. B **525**, 143 (2002) [hep-ph/0110072].
- [23] M. Fujii and K. Hamaguchi, Phys. Rev. D **66**, 083501 (2002) [hep-ph/0205044].
- [24] M. Fujii and T. Yanagida, Phys. Lett. B **542**, 80 (2002) [hep-ph/0206066].
- [25] L. Roszkowski and O. Seto, Phys. Rev. Lett. **98**, 161304 (2007) [hep-ph/0608013].
- [26] O. Seto and M. Yamaguchi, Phys. Rev. D **75**, 123506 (2007) [arXiv:0704.0510 [hep-ph]].
- [27] I. M. Shoemaker and A. Kusenko, Phys. Rev. D **80**, 075021 (2009).
- [28] F. Doddato and J. McDonald, JCAP **1106**, 008 (2011) [arXiv:1101.5328 [hep-ph]].
- [29] S. Kasuya and M. Kawasaki, Phys. Rev. D **84**, 123528 (2011) [arXiv:1107.0403 [hep-ph]].
- [30] F. Doddato and J. McDonald, JCAP **1307**, 004 (2013) [arXiv:1211.1892 [hep-ph]].
- [31] S. Kasuya, M. Kawasaki and M. Yamada, Phys. Lett. B **726**, 1 (2013) [arXiv:1211.4743 [hep-ph]].
- [32] A. Kamada, M. Kawasaki and M. Yamada, Phys. Lett. B **719**, 9 (2013) [arXiv:1211.6813 [hep-ph]].
- [33] K. Harigaya, M. Kawasaki, K. Mukaida and M. Yamada, to be published in PRD, arXiv:1402.2846 [hep-ph].
- [34] R. Allahverdi and M. Drees, Phys. Rev. Lett. **89**, 091302 (2002) [hep-ph/0203118]; R. Allahverdi and M. Drees, Phys. Rev. D **66**, 063513 (2002) [hep-ph/0205246].
- [35] T. Moroi, M. Yamaguchi and T. Yanagida, Phys. Lett. B **342**, 105 (1995) [hep-ph/9409367].
- [36] M. Kawasaki, T. Moroi and T. Yanagida, Phys. Lett. B **370**, 52 (1996) [hep-ph/9509399].
- [37] T. Moroi and L. Randall, Nucl. Phys. B **570**, 455 (2000) [hep-ph/9906527].
- [38] G. B. Gelmini and P. Gondolo, Phys. Rev. D **74**, 023510 (2006) [hep-ph/0602230].
- [39] Y. Kurata and N. Maekawa, Prog. Theor. Phys. **127**, 657 (2012) [arXiv:1201.3696 [hep-ph]].
- [40] T. Moroi, H. Murayama and M. Yamaguchi, Phys. Lett. B **303**, 289 (1993).
- [41] T. Gherghetta, C. F. Kolda and S. P. Martin, Nucl. Phys. B **468**, 37 (1996) [hep-ph/9510370].

- [42] A. D. Sakharov, Pisma Zh. Eksp. Teor. Fiz. **5**, 32 (1967) [JETP Lett. **5**, 24 (1967)] [Sov. Phys. Usp. **34**, 392 (1991)] [Usp. Fiz. Nauk **161**, 61 (1991)].
- [43] V. A. Kuzmin, V. A. Rubakov and M. E. Shaposhnikov, Phys. Lett. B **155**, 36 (1985).
- [44] M. Kawasaki, M. Yamaguchi and T. Yanagida, Phys. Rev. Lett. **85**, 3572 (2000) [hep-ph/0004243].
- [45] R. Kallosh and A. Linde, JCAP **1011**, 011 (2010) [arXiv:1008.3375 [hep-th]].
- [46] M. Fukugita and T. Yanagida, Phys. Lett. B **174**, 45 (1986).
- [47] G. Hinshaw *et al.* [WMAP Collaboration], Astrophys. J. Suppl. **208**, 19 (2013) [arXiv:1212.5226 [astro-ph.CO]].
- [48] P. A. R. Ade *et al.* [Planck Collaboration], arXiv:1303.5076 [astro-ph.CO].
- [49] P. A. R. Ade *et al.* [Planck Collaboration], arXiv:1303.5082 [astro-ph.CO].
- [50] J. Beringer *et al.* [Particle Data Group Collaboration], Phys. Rev. D **86**, 010001 (2012).
- [51] R. Allahverdi and A. Mazumdar, JCAP **0610**, 008 (2006) [hep-ph/0512227].
- [52] T. Hiramatsu, M. Kawasaki and F. Takahashi, JCAP **1006**, 008 (2010) [arXiv:1003.1779 [hep-ph]].
- [53] M. Kawasaki and M. Yamada, Phys. Rev. D **87**, 023517 (2013) [arXiv:1209.5781 [hep-ph]].
- [54] D. J. H. Chung, E. W. Kolb and A. Riotto, Phys. Rev. D **60**, 063504 (1999) [hep-ph/9809453].
- [55] K. Mukaida and K. Nakayama, JCAP **1301**, 017 (2013) [JCAP **1301**, 017 (2013)] [arXiv:1208.3399 [hep-ph]].
- [56] K. Griest and D. Seckel, Phys. Rev. D **43**, 3191 (1991).
- [57] P. Gondolo and G. Gelmini, Nucl. Phys. B **360**, 145 (1991).
- [58] J. R. Ellis, T. Falk and K. A. Olive, Phys. Lett. B **444**, 367 (1998) [hep-ph/9810360].
- [59] G. F. Giudice, E. W. Kolb and A. Riotto, Phys. Rev. D **64**, 023508 (2001) [hep-ph/0005123].
- [60] A. Kurkela and G. D. Moore, JHEP **1112**, 044 (2011) [arXiv:1107.5050 [hep-ph]].
- [61] K. Harigaya and K. Mukaida, arXiv:1312.3097 [hep-ph].
- [62] S. Davidson and S. Sarkar, JHEP **0011**, 012 (2000) [hep-ph/0009078].
- [63] P. B. Arnold, G. D. Moore and L. G. Yaffe, JHEP **0301**, 030 (2003) [hep-ph/0209353].
- [64] P. Jaikumar and A. Mazumdar, Nucl. Phys. B **683**, 264 (2004) [hep-ph/0212265].
- [65] L. D. Landau and I. Pomeranchuk, Dokl. Akad. Nauk SSSR. **92**, 535 (1953).
- [66] A. B. Migdal, Phys. Rev. **103**, 1811 (1956).
- [67] M. Gyulassy and X. -n. Wang, Nucl. Phys. B **420**, 583 (1994) [nucl-th/9306003].

- [68] P. B. Arnold, G. D. Moore and L. G. Yaffe, JHEP **0111**, 057 (2001) [hep-ph/0109064].
- [69] P. B. Arnold, G. D. Moore and L. G. Yaffe, JHEP **0112**, 009 (2001) [hep-ph/0111107].
- [70] P. B. Arnold, G. D. Moore and L. G. Yaffe, JHEP **0206**, 030 (2002) [hep-ph/0204343].
- [71] D. Besak and D. Bodeker, JHEP **1005**, 007 (2010) [arXiv:1002.0022 [hep-ph]].
- [72] F. Takahashi, Phys. Lett. B **693**, 140 (2010) [arXiv:1006.2801 [hep-ph]]; K. Nakayama and F. Takahashi, JCAP **1011**, 009 (2010) [arXiv:1008.2956 [hep-ph]].
- [73] K. Harigaya, M. Ibe, K. Schmitz and T. T. Yanagida, Phys. Lett. B **720**, 125 (2013) [arXiv:1211.6241 [hep-ph]]; arXiv:1403.4536 [hep-ph].
- [74] E. Aprile [XENON1T Collaboration], arXiv:1206.6288 [astro-ph.IM].
- [75] ATLAS-CONF-2013-047 [ATLAS Collaboration].
- [76] A. Kamada, M. Kawasaki and M. Yamada, in preparation.
- [77] A. de Gouvêa, T. Moroi and H. Murayama, Phys. Rev. D **56**, 1281 (1997).
- [78] M. Fujii, K. Hamaguchi and T. Yanagida, Phys. Rev. D **65**, 043511 (2002) [hep-ph/0109154].
- [79] M. Bolz, A. Brandenburg and W. Buchmuller, Nucl. Phys. B **606**, 518 (2001) [Erratum-ibid. B **790**, 336 (2008)] [hep-ph/0012052].
- [80] J. Pradler and F. D. Steffen, Phys. Rev. D **75**, 023509 (2007) [hep-ph/0608344].
- [81] A. Kusenko, F. Takahashi and T. T. Yanagida, Phys. Lett. B **693**, 144 (2010) [arXiv:1006.1731 [hep-ph]].
- [82] Y. Mambrini, K. A. Olive, J. Quevillon and B. Zaldivar, Phys. Rev. Lett. **110**, 241306 (2013) [arXiv:1302.4438 [hep-ph]].
- [83] J. L. Feng, S. Su and F. Takayama, Phys. Rev. D **70**, 075019 (2004) [hep-ph/0404231].
- [84] T. Moroi and N. Yokozaki, Phys. Lett. B **701**, 568 (2011) [arXiv:1105.3294 [hep-ph]].
- [85] K. Jedamzik, M. Lemoine and G. Moulhaka, JCAP **0607**, 010 (2006) [astro-ph/0508141].
- [86] F. D. Steffen, JCAP **0609**, 001 (2006) [hep-ph/0605306].
- [87] M. Viel, G. D. Becker, J. S. Bolton and M. G. Haehnelt, Phys. Rev. D **88**, 043502 (2013) [arXiv:1306.2314 [astro-ph.CO]].
- [88] M. Sitwell, A. Mesinger, Y. -Z. Ma and K. Sigurdson, arXiv:1310.0029 [astro-ph.CO].
- [89] M. Kawasaki, K. Kohri and T. Moroi, Phys. Rev. D **71**, 083502 (2005) [astro-ph/0408426].
- [90] M. Kawasaki, K. Kohri, T. Moroi and A. Yotsuyanagi, Phys. Rev. D **78**, 065011 (2008) [arXiv:0804.3745 [hep-ph]].

- [91] G. R. Dvali, A. Kusenko and M. E. Shaposhnikov, Phys. Lett. B **417**, 99 (1998) [hep-ph/9707423].
- [92] F. Doddato and J. McDonald, JCAP **1206**, 031 (2012) [arXiv:1111.2305 [hep-ph]].
- [93] S. Kasuya and M. Kawasaki, Phys. Rev. Lett. **85**, 2677 (2000) [hep-ph/0006128].
- [94] J. Hisano, M. M. Nojiri and N. Okada, Phys. Rev. D **64**, 023511 (2001) [hep-ph/0102045].
- [95] M. Laine and M. E. Shaposhnikov, Nucl. Phys. B **532**, 376 (1998) [hep-ph/9804237].
- [96] R. Banerjee and K. Jedamzik, Phys. Lett. B **484**, 278 (2000) [hep-ph/0005031].